AD-A089 703   SYRACUSE UNIV NY   DEPT OF ELECTRICAL AND COMPUTER EN--ETC   F/G 20/3
AN IMPROVED E-FIELD SOLUTION FOR A CONDUCTING BODY OF REVOLUTIO--ETC(U)
JUN 80   J R MAUTZ, R F HARRINGTON   F30602-79-C-0011

UNCLASSIFIED   RADC-TR-80-194   NL

END
DATE
FILMED
11-80
DTIC

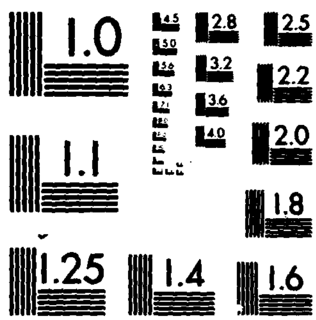
1.0
2.8
2.5
3.2
2.2
3.6
4.0
2.0
1.1
1.8
1.25
1.4
1.6

FOR THE COMMANDER:

Acting Chief, Plans Office

SUBJECT TO EXPORT CONTROL LAWS

UNCLASSIFIED

SECURITY CLASSIFICATION OF THIS PAGE (When Data Entered)

## REPORT DOCUMENTATION PAGE

READ INSTRUCTIONS BEFORE COMPLETING FORM

| | |
|---|---|
| 1. REPORT NUMBER: RADC-TR-80-194 | 2. GOVT ACCESSION NO.: AD-A089 |
| 3. RECIPIENT'S CATALOG NUMBER: 703 | |
| 4. TITLE (and Subtitle): AN IMPROVED E-FIELD SOLUTION FOR A CONDUCTING BODY OF REVOLUTION | 5. TYPE OF REPORT & PERIOD COVERED: Phase Rep[illegible]t |
| | 6. PERFORMING ORG. REPORT NUMBER: N/A |
| 7. AUTHOR(s): Joseph R. Mautz, Roger F. Harrington | 8. CONTRACT OR GRANT NUMBER(s): F30602-79-C-0011 |
| 9. PERFORMING ORGANIZATION NAME AND ADDRESS: Syracuse University, Department of Electrical and Computer Engineering, Syracuse NY 13210 | 10. PROGRAM ELEMENT, PROJECT, TASK AREA & WORK UNIT NUMBERS: 62702F, 23380317 |
| 11. CONTROLLING OFFICE NAME AND ADDRESS: Rome Air Development Center (RBCT), Griffiss AFB NY 13441 | 12. REPORT DATE: Jun[illegible]80 |
| | 13. NUMBER OF PAGES: 78 |
| 14. MONITORING AGENCY NAME & ADDRESS (if different from Controlling Office): Same | 15. SECURITY CLASS. (of this report): UNCLASSIFIED |
| | 15a. DECLASSIFICATION/DOWNGRADING SCHEDULE: N/A |

16. DISTRIBUTION STATEMENT (of this Report)

Approved for public release; distribution unlimited.

17. DISTRIBUTION STATEMENT (of the abstract entered in Block 20, if different from Report)

Same

18. SUPPLEMENTARY NOTES

RADC Project Engineer: Roy F. Stratton (RBCT)

19. KEY WORDS (Continue on reverse side if necessary and identify by block number)

Body of revolution
Computer program
E-Field solution
Method of moments

20. ABSTRACT (Continue on reverse side if necessary and identify by block number)

The electric field integro-differential equation for electromagnetic scattering from a perfectly conducting body of revolution is solved by the method of moments. A numerical solution is obtained by means of a computer program which is described and listed. This computer program is designed to handle oblique plane wave incidence efficiently. Spatial staggering of expansion functions for the orthogonal components of the induced current is known to give good accuracy over

(Cont'd)

DD FORM 1 JAN 73 1473 EDITION OF 1 NOV 65 IS OBSOLETE

UNCLASSIFIED

SECURITY CLASSIFICATION OF THIS PAGE (When Data Entered)

406737

Item 20 (Cont'd)

when the body of revolution has edges. By means of triangle and pulse expansion functions, this spatial staggering is achieved without the use of shifted source segments. The present computer program is highly competitive with other available programs as concerns storage, execution time, and accuracy.

CONTENTS

## LIST OF TABLES



## LIST OF FIGURES

PART ONE

SOLUTION PROCEDURE AND NUMERICAL RESULTS

## I. INTRODUCTION

The purpose of this report is to develop an efficient numerical solution to the E-field integro-differential equation for electromagnetic excitation of a perfectly conducting body of revolution. This numerical solution is obtained by applying the method of moments to the E-field equation. The E-field equation states that the tangential component of the total electric field is zero on the surface S of the body of revolution.

The problem is stated in Section II of [1] and the solution is similar to that in Section IV of [1]. Except where otherwise indicated, the notation is the same as in [1]. Equation numbers drawn from [1] are preceded by 1-. For instance, (1-40) denotes equation (40) of reference [1].

The following differences exist between the present solution and that in [1]. In the present solution, the approximation to the generating curve of the body of revolution consists of half as many straight line segments as in [1]. Otherwise, the t directed expansion functions are the same as those in [1]. However, for $\phi$ directed expansion functions, the pulses used in [2] are adopted. Here, t is the arc length along the generating curve and $\phi$ is the azimuthal angle. The testing functions are the complex conjugates of the expansion functions. For calculation of the elements of the moment matrix, each integral with respect to t' over each straight line segment is evaluated by using $n_t$-point Gaussian quadrature

and each integral with respect to t over each straight line segment is approximated by sampling at the midpoint of the line segment. Although t and t' are both arc lengths along the generating curve, t denotes integration over a testing function and t' denotes integration over an expansion function. The former integration is called a field integration, the latter a source integration. As in [1], $n_\phi$-point Gaussian quadrature is used for the integration with respect to $\phi$. However, the method [3] of eliminating the singularity is used to fortify the Gaussian quadrature integrations with respect to t' and $\phi$ whenever the source segment is sufficiently close to the field point. For calculation of the elements of the excitation vector, $n_T$-point Gaussian quadrature is used for the t integration.

With regard to $\phi$ directed testing, calculation of the moment matrix by sampling the t integrand at the center of each straight line segment is equivalent to point matching. However, for t directed testing, this calculation can not be viewed as simple point matching because each t directed testing function extends over two intervals and therefore must be represented by two Dirac delta functions instead of one. Furthermore, the electric charge associated with each t directed testing function is also represented by two Dirac delta functions.

The method of solution formulated in Part One of this report is implemented by the computer program described and listed in Part Two. The present computer program takes almost twice as long to compile as that in [1]. However, for axial incidence and for moment matrices of roughly the same order, the present program with $n_t = n_T = 2$ and $n_\phi = 20$ executes almost as fast as that in [1] with $N_\phi = 20$. For moment matrices of the

same order, the present computer program probably executes faster than that in [2] because the one in [2] uses twice as many source segments and twice as many field points. For oblique incidence, several moment matrices are required. The computer program in [1] calculates the moment matrices one by one, that is, each moment matrix is calculated from scratch. However, the present computer program takes advantage of the fact that some intermediate calculations are common to all the moment matrices. Hence, if there is room enough to store all the moment matrices simultaneously, the present computer program should execute much faster for oblique incidence. Results obtained from the present computer program are generally more accurate than those obtained from [1], especially for bodies of revolution with edges.

## II. METHOD OF MOMENTS SOLUTION

The boundary condition that the tangential component of the total electric field is zero on S is expressed by (1-40) and supporting equations (1-41)-(1-43). Following the method of moments, we approximate the electric current $\underline{J}$ on S by

$$\underline{J} = \sum_{n,j} \left( I^t_{nj} \underline{J}^t_{nj} + I^\phi_{nj} \underline{J}^\phi_{nj} \right) \tag{1}$$

and substitute this $\underline{J}$ into (1-41). In (1), $\underline{J}^t_{nj}$ and $\underline{J}^\phi_{nj}$ are known expansion functions and $I^t_{nj}$ and $I^\phi_{nj}$ are unknown coefficients to be determined.

The expansion functions $\underline{J}^t_{nj}$ and $\underline{J}^\phi_{nj}$ are defined by

$$\underline{J}^t_{nj} = \underline{u}_t \frac{T_j(t)}{\rho} e^{jn\phi} \qquad \begin{array}{l} j = 1,2, \ldots P-2 \\ n = 0, \pm 1, \pm 2, \ldots \end{array} \tag{2}$$

$$\underline{J}^\phi_{nj} = \underline{u}_\phi \frac{P_j(t)}{\rho_j} e^{jn\phi} \qquad \begin{array}{l} j = 1,2, \ldots P-1 \\ n = 0, \pm 1, \pm 2, \ldots \end{array} \tag{3}$$

where $\underline{u}_t$ and $\underline{u}_\phi$ are unit vectors in the t and $\phi$ directions, respectively. The j which appears in the argument of the exponential in (2) and (3) is not to be confused with the j which appears elsewhere in (2) and (3). The former j is $\sqrt{-1}$ and the latter j is the subscript which goes from 1 to either P-2 or P-1. The function $T_j(t)$ is the triangle function shown in Fig. 1 and $\rho$ is the distance from the axis of the body of revolution. The function $P_j(t)$ is the pulse function shown in Fig. 2 and $\rho_j$ is the value of $\rho$ at $t = t_j$ where $t_j$ is the center point of the domain of the pulse. The purpose of the scale factor $1/\rho_j$ in (3) is to give (3) the same dimension as (2), namely, 1/length. The pulse doublet $\frac{d}{dt} T_j(t)$ in Fig. 3 is

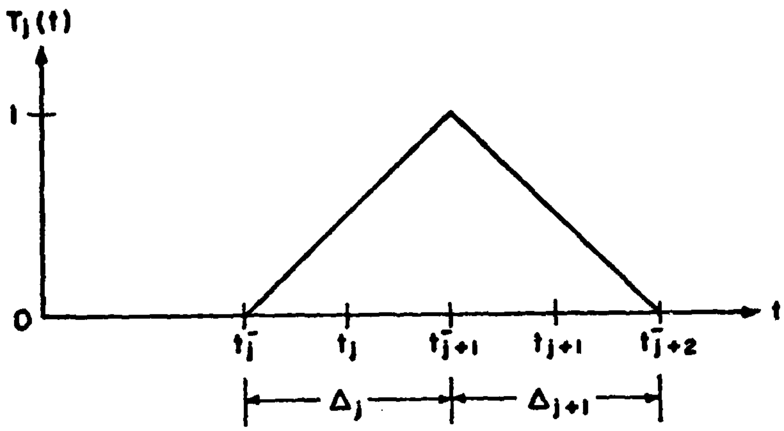


Fig. 1. Triangle function $T_j(t)$.

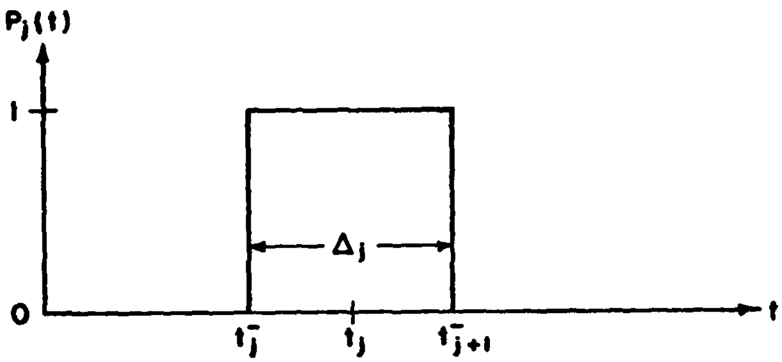


Fig. 2. Pulse function $P_j(t)$.

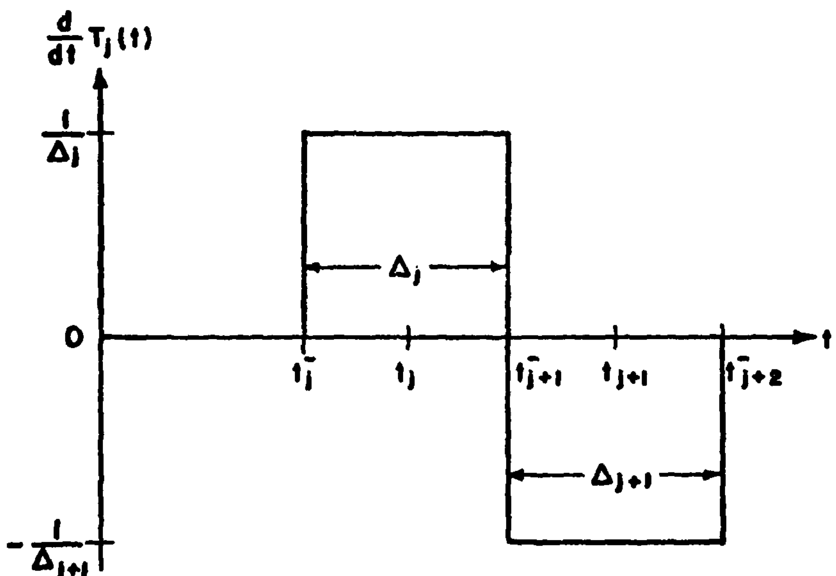


Fig. 3. Pulse doublet $\frac{d}{dt} T_j(t)$.

used later on in the method of moments solution. In Figs. 1, 2, and 3, t is the arc length along the generating curve. It is assumed that the generating curve consists of P-1 straight line segments where P is an odd integer greater than or equal to 3. The jth such segment extends from $t_j^-$ to $t_{j+1}^-$. Its length is $\Delta_j$. The expansion functions (2) and (3) are especially appropriate if the body of revolution is an infinitely thin perfectly conducting surface with edges at both ends of the generating curve. This is true because the t directed electric current is supposed to approach zero at an edge whereas the $\phi$ directed electric current might grow large there [4].

Testing functions $\underline{W}_{ni}^{t}$ and $\underline{W}_{ni}^{\phi}$ are defined by

$$\underline{W}_{ni}^{t} = \underline{u}_t \frac{T_i(t)}{\rho} e^{-jn\phi} \qquad \begin{array}{l} i = 1,2, \ldots P-2 \\ n = 0, \pm 1, \pm 2, \ldots \end{array} \tag{4}$$

$$\underline{W}_{ni}^{\phi} = \underline{u}_\phi \frac{P_i(t)}{\rho_i} e^{-jn\phi} \qquad \begin{array}{l} i = 1,2, \ldots P-1 \\ n = 0, \pm 1, \pm 2, \ldots \end{array} \tag{5}$$

After substitution of (1) into (1-41), the dot product of (1-41) is taken with each testing function. These dot products are then integrated over S. As can be derived by retracing the development (1-40)-(1-65) with (1-46) and (1-47) replaced by (2)-(5), the resulting matrix equation is

$$\begin{bmatrix} Z_n^{tt} & Z_n^{t\phi} \\ Z_n^{\phi t} & Z_n^{\phi\phi} \end{bmatrix} \begin{bmatrix} \vec{I}_n^{t} \\ \vec{I}_n^{\phi} \end{bmatrix} = \begin{bmatrix} \vec{V}_n^{t} \\ \vec{V}_n^{\phi} \end{bmatrix}, \quad n = 0, \pm 1, \pm 2, \ldots \tag{6}$$

where the $Z_n$'s are submatrices and the $\vec{I}_n$'s and $\vec{V}_n$'s are column vectors.

The matrix of the $Z_n$'s on the left-hand side of (6) is a square matrix called the moment matrix. The column vector on the right-hand side of (6) is called the excitation vector. The jth element of $\vec{I}_n^t$ is $I_{nj}^t$ and that of $\vec{I}_n^\phi$ is $I_{nj}^\phi$. The ith elements of $\vec{V}_n^t$ and $\vec{V}_n^\phi$ are given by

$$V_{ni}^t = \frac{1}{\eta} \iint_S \underline{W}_{ni}^t \cdot \underline{E}^i dS\ , \quad i = 1,2, \ldots P-2 \tag{7}$$

$$V_{ni}^\phi = \frac{1}{\eta} \iint_S \underline{W}_{ni}^\phi \cdot \underline{E}^i dS\ , \quad i = 1,2, \ldots P-1 \tag{8}$$

where $\eta$ is the intrinsic impedance and $\underline{E}^i$ is the incident electric field. The ijth elements of the $Z_n$'s are given by

$$(Z_n^{tt})_{ij} = j \int_{\bar{t}_i}^{\bar{t}_{i+2}} dt \int_{\bar{t}_j}^{\bar{t}_{j+2}} dt' \{k^2 T_i(t)\ T_j(t')(G_5 \sin v \sin v'$$

$$+ G_7 \cos v \cos v') - G_7 \frac{d}{dt} T_i(t) \frac{d}{dt'} T_j(t')\} \tag{9}$$

$$(Z_n^{\phi t})_{ij} = -\frac{1}{\rho_i} \int_{\bar{t}_i}^{\bar{t}_{i+1}} dt\ P_i(t) \int_{\bar{t}_j}^{\bar{t}_{j+2}} dt' (k^2 \rho\ T_j(t') G_6 \sin v' + nG_7 \frac{d}{dt'} T_j(t')) \tag{10}$$

$$(Z_n^{t\phi})_{ij} = \frac{1}{\rho_j} \int_{\bar{t}_i}^{\bar{t}_{i+2}} dt \int_{\bar{t}_j}^{\bar{t}_{j+1}} dt'\ P_j(t')(k^2 \rho' T_i(t)\ G_6 \sin v + nG_7 \frac{d}{dt} T_i(t)) \tag{11}$$

$$(Z_n^{\phi\phi})_{ij} = \frac{j}{\rho_i \rho_j} \int_{\bar{t}_i}^{\bar{t}_{i+1}} dt\ P_i(t) \int_{\bar{t}_j}^{\bar{t}_{j+1}} dt' P_j(t')(k^2 \rho\rho' G_5 - n^2 G_7) \tag{12}$$

where

$$G_7 = G_4 + G_5 \tag{13}$$

$$G_4 = 2 \int_0^{\pi} d\phi \, \frac{e^{-jkR}}{kR} \sin^2(\frac{\phi}{2}) \cos (n\phi) \tag{14}$$

$$G_5 = \int_0^{\pi} d\phi \, \frac{e^{-jkR}}{kR} \cos \phi \cos (n\phi) \tag{15}$$

$$G_6 = \int_0^{\pi} d\phi \, \frac{e^{-jkR}}{kR} \sin \phi \sin (n\phi) \tag{16}$$

$$R = \sqrt{(\rho'-\rho)^2 + (z'-z)^2 + 4\rho\rho'\sin^2 (\frac{\phi}{2})} \tag{17}$$

Here, k is the propagation constant, $\rho$ is the distance from the axis of the body of revolution, z is the rectangular coordinate along this axis, and v is the angle that the tangent to the generating curve makes with the z axis. The angle v is positive if $\rho$ increases with t and negative otherwise. The parameters $\rho$, z, and v depend on t. Their counterparts $\rho'$, z', and v' depend on t'. The ranges of values of i and j in (9)-(12) are such that the regions of integration therein move from one end of the generating curve to the other end. It is understood that $n = 0, \pm 1, \pm 2, \ldots$ in (7)-(16).

Note that the quantity $G_4$ defined by (14) is different from that defined by (1-62). The trigonometric identity

$$1 = 2 \sin^2(\frac{\phi}{2}) + \cos \phi \tag{18}$$

was used to express (1-62) as the sum of (14) and (15). Expression (14) is more suitable for computation than (1-62) because the integrand in (14) is always finite.

## III. EVALUATION OF THE MOMENT MATRIX

One by one evaluation of the elements (9)-(12) of the moment matrix is inefficient because of the overlapping regions of integration. For instance, both $(Z_n^{tt})_{i-1,j}$ and $(Z_n^{tt})_{ij}$ contain integrals with respect to t over the ith segment $(t_i^-, t_{i+1}^-)$. If $(Z_n^{tt})_{i-1,j}$ and $(Z_n^{tt})_{ij}$ are calculated one after the other, these integrals must either be stored or calculated twice.

In this report, the contributions to (9)-(12) are accounted for by regions of integration rather than by matrix elements. Consider the contributions due to the 2-dimensional region of integration

$$t_p^- \leq t \leq t_{p+1}^-$$
$$t_q^- \leq t' \leq t_{q+1}^- \quad .$$

This region of integration is called $A_{pq}$. Integrations in (9)-(12) are carried out over $A_{pq}$ for $\{\substack{i=p \\ j=q}\}$ or possibly $\{\substack{i=p-1 \\ j=q}\}$ , $\{\substack{i=p \\ j=q-1}\}$ and $\{\substack{i=p-1 \\ j=q-1}\}$. For all other values of i and j, no region of integration in (9)-(12) intersects $A_{pq}$. Setting $\{\substack{i=p-1 \\ j=q-1}\}$ , $\{\substack{i=p \\ j=q-1}\}$ , $\{\substack{i=p-1 \\ j=q}\}$, and $\{\substack{i=p \\ j=q}\}$ successively in (9)-(12) and counting only the region of integration $A_{pq}$, we obtain

$$(\overset{*}{Z}{}_n^{tt})_{ij} = j \int_{t_p^-}^{t_{p+1}^-} dt \int_{t_q^-}^{t_{q+1}^-} dt' \{k^2 T_i(t) T_j(t') (G_5 \sin v \sin v' + G_7 \cos v \cos v') -$$
$$- G_7 \frac{d}{dt} T_i(t) \frac{d}{dt'} T_j(t')\} \tag{19}$$

$$(\overset{*}{Z}{}_n^{\phi t})_{pj} = - \frac{1}{\rho_p} \int_{t_p^-}^{t_{p+1}^-} dt \, P_p(t) \int_{t_q^-}^{t_{q+1}^-} dt' (k^2 \rho \, T_j(t') \, G_6 \sin v' + nG_7 \frac{d}{dt'} T_j(t')) \tag{20}$$

$$(\overset{*}{Z}{}_n^{t\phi})_{iq} = \frac{1}{\rho_q}\int_{\bar{t}_p}^{\bar{t}_{p+1}} dt \int_{\bar{t}_q}^{\bar{t}_{q+1}} dt' P_q(t')(k^2\rho' \; T_i(t) G_6 \sin v + nG_7 \frac{d}{dt} T_i(t)) \tag{21}$$

$$(Z_n^{\phi\phi})_{pq} = \frac{j}{\rho_p\rho_q}\int_{\bar{t}_p}^{\bar{t}_{p+1}} dt \; P_p(t) \int_{\bar{t}_q}^{\bar{t}_{q+1}} dt' P_q(t') \; (k^2\rho\rho' G_5 - n^2 G_7) \tag{22}$$

In (19) and (21),

$$\begin{aligned} i &= p-1,\ p \\ i &\neq 0 \\ i &\neq P-1 \end{aligned} \tag{23}$$

In (19) and (20),

$$\begin{aligned} j &= q-1,\ q \\ j &\neq 0 \\ j &\neq P-1 \end{aligned} \tag{24}$$

The asterisk ($^*$) on the left-hand sides of (19)-(21) denotes the contribution due to integration over the region $A_{pq}$. Note that (22) is (12) with ij replaced by pq. Because (12) has no overlapping regions of integration, it is not affected by the change from calculation by matrix elements to calculation by regions of integration.

Next, each integral with respect to t in (19)-(22) is evaluated by using the approximation

$$\int_{\bar{t}_p}^{\bar{t}_{p+1}} f(t)dt = f(t_p)\ \Delta_p \tag{25}$$

where f(t) is the relevant integrand and, as indicated in Figs. 1, 2, and 3,

$$t_p = \frac{1}{2}(t_p^- + t_{p+1}^-) \tag{26}$$

$$\Delta_p = t_{p+1}^- - t_p^- \tag{27}$$

Application of (25) to each integral with respect to t in (19)-(22) gives

$$(\overset{*}{Z}{}_n^{tt})_{ij} = j\Delta_p \int_{t_q^-}^{t_{q+1}^-} dt'\{k^2 T_i(t_p) T_j(t')(G_5 \sin v_p \sin v' + G_7 \cos v_p \cos v') - $$
$$- G_7 [\frac{d}{dt} T_i(t)]_{t_p} \frac{d}{dt'} T_j(t')\} \tag{28}$$

$$(\overset{*}{Z}{}_n^{\phi t})_{pj} = - \Delta_p P_p(t_p) \int_{t_q^-}^{t_{q+1}^-} dt'(k^2 T_j(t') G_6 \sin v' + \frac{n}{\rho_p} G_7 \frac{d}{dt'} T_j(t')) \tag{29}$$

$$(\overset{*}{Z}{}_n^{t\phi})_{iq} = \Delta_p \int_{t_q^-}^{t_{q+1}^-} dt' \, P_q(t')(\frac{k^2 \rho'}{\rho_q} T_i(t_p) G_6 \sin v_p + \frac{n}{\rho_q} G_7 [\frac{d}{dt} T_i(t)]_{t_p}) \tag{30}$$

$$(Z_n^{\phi\phi})_{pq} = j\Delta_p \, P_p(t_p) \int_{t_q^-}^{t_{q+1}^-} dt' P_q(t')(\frac{k^2 \rho'}{\rho_q} G_5 - \frac{n^2}{\rho_p \rho_q} G_7) \tag{31}$$

where $v_p$ is the value of v at $t = t_p$. Incidentally, $v = v_p$ for $t_p^- < t < t_{p+1}^-$ because the generating curve was assumed to be straight there. In (28)-(31), $G_5$, $G_6$, and $G_7$ are given, respectively, by (15), (16), and (13) with R replaced by $R_p$ where

$$R_p = \sqrt{(\rho'-\rho_p)^2 + (z'-z_p)^2 + 4\rho_p \rho' \sin^2 (\frac{\phi}{2})} \tag{32}$$

where $z_p$ is the value of z at $t = t_p$. The range of values of i and j

in (28)-(30) is, as inherited from (19)-(21), given by (23) and (24).

Application of (25) is only one way to obtain (28)-(31). Another way to obtain (28)-(31) is by approximating the G's in (19)-(22) by their values at $t = t_p$. This amounts to immediate rather than consequential replacement of R by $R_p$ in (14)-(16). A third way to obtain (28)-(31) is by substituting the approximation

$$T_i(t) \approx \frac{1}{2} (\Delta_i \delta(t-t_i) + \Delta_{i+1} \delta(t-t_{i+1})) \tag{33}$$

$$P_p(t) \approx \Delta_p \delta(t-t_p) \tag{34}$$

$$\frac{d}{dt} T_i(t) \approx \delta(t-t_i) - \delta(t-t_{i+1}) \tag{35}$$

into (19)-(22). Here, $\delta(t)$ is the Dirac delta function. The approximation (33) preserves the value of the surface integral of the t component of the t directed electric current (4) on the portion of S for which

$$t_p^- \le t \le t_{p+1}^- , \quad p = 1,2, \ldots P-1$$

$$\phi_a \le \phi \le \phi_b$$

where $\phi_a$ and $\phi_b$ are arbitrary. Likewise, the approximations (34) and (35) do not alter the values of such surface integrals of the electric current (5) and the electric charge associated with either (4) or (5).

Equations (28)-(31) were obtained by using the testing functions (4) and (5) and invoking either the approximation (25) or the set of approximations (33)-(35). Can a set of effective testing functions be defined such that (28)-(31) can be obtained by using these functions and no auxiliary approximation? Testing functions could be defined by substituting (33)

and (34) into (4) and (5), but the approximation (35) would still be required in order to obtain (28)-(31). Unfortunately, the approximation (35) is not consistent with the approximation (33). Hence, it is not possible to trace (28)-(31) to effective testing functions.

The functions $P_q(t')$, $T_j(t')$, $\frac{d}{dt'} T_j(t')$, $v'$, and $\rho'$ in (28)-(31) are given by

$$P_q(t') = 1 \tag{36}$$

$$T_j(t') = \frac{1}{2} + \frac{(-1)^{q-j}(t'-t_q)}{\Delta_q}, \quad j = q-1, q \tag{37}$$

$$\frac{d}{dt'} T_j(t') = \frac{(-1)^{q-j}}{\Delta_q}, \quad j = q-1, q \tag{38}$$

$$v' = v_q \tag{39}$$

$$\rho' = \rho_q + (t'-t_q)\sin v_q \tag{40}$$

for $t_q^- < t' < t_{q+1}^-$. Equations (36)-(38) can be obtained from Figs. 1,2, and 3. Equations (39) and (40) are true because the generating curve is straight for $t_q^- < t' < t_{q+1}^-$. Replacement of j, q, and t' by i, p, and $t_p$ in (36)-(38) gives

$$P_p(t_p) = 1 \tag{41}$$

$$T_i(t_p) = \frac{1}{2} \tag{42}$$

$$\left[\frac{d}{dt} T_i(t)\right]_{t_p} = \frac{(-1)^{p-i}}{\Delta_p} \tag{43}$$

Substitution of (36)-(43) into (28)-(31) yields

$$(\overset{*}{Z}{}^{tt}_n)_{ij} = j\Delta_p \int_{t_q^-}^{t_{q+1}^-} dt'\{\frac{k^2}{4}\left(1 + \frac{(-1)^{q-j}2(t'-t_q)}{\Delta_q}\right)(G_5 \sin v_p \sin v_q + G_7 \cos v_p \cos v_q) - \frac{(-1)^{p+q-i-j}G_7}{\Delta_p \Delta_q}\} \tag{44}$$

$$(\overset{*}{Z}{}^{\phi t}_n)_{pj} = -\Delta_p \int_{t_q^-}^{t_{q+1}^-} dt'\left(\frac{k^2}{2}\left(1 + \frac{(-1)^{q-j}2(t'-t_q)}{\Delta_q}\right)G_6 \sin v_q + \frac{(-1)^{q-j}nG_7}{\rho_p \Delta_q}\right) \tag{45}$$

$$(\overset{*}{Z}{}^{t\phi}_n)_{iq} = \Delta_p \int_{t_q^-}^{t_{q+1}^-} dt' \left(\frac{k^2}{2}\left(1 + \frac{(t'-t_q)}{\rho_q} \sin v_q\right)G_6 \sin v_p + \frac{(-1)^{p-i}nG_7}{\rho_q \Delta_p}\right) \tag{46}$$

$$(Z^{\phi\phi}_n)_{pq} = j\Delta_p \int_{t_q^-}^{t_{q+1}^-} dt'\left(k^2\left(1 + \frac{(t'-t_q)}{\rho_q} \sin v_q\right)G_5 - \frac{n^2}{\rho_p \rho_q} G_7\right) \tag{47}$$

Equations (42)-(45) are rewritten as

$$(\overset{*}{Z}{}^{tt}_n)_{ij} = \frac{j\, k^2 \Delta_p \Delta_q}{8}(G_{5a} \sin v_p \sin v_q + G_{7a} \cos v_p \cos v_q) + \frac{(-1)^{q-j} j k^2 \Delta_p \Delta_q}{8}(G_{5b} \sin v_p \sin v_q + G_{7b} \cos v_p \cos v_q) - -(-1)^{p+q-i-j} \frac{j}{2} G_{7a} \tag{48}$$

$$(\overset{*}{Z}{}^{\phi t}_n)_{pj} = -\left(\frac{k^2 \Delta_p \Delta_q \sin v_q}{4}\right)G_{6a} - (-1)^{q-j}\{\left(\frac{k^2 \Delta_p \Delta_q \sin v_q}{4}\right)G_{6b} + \left(\frac{n\Delta_p}{2\rho_p}\right)G_{7a}\} \tag{49}$$

$$(\overset{*}{Z}{}_n^{t\phi})_{iq} = \left(\frac{k^2\Delta_p\Delta_q \sin v_p}{4}\right)\left(G_{6a} + \frac{\Delta_q \sin v_q}{2\rho_q} G_{6b}\right) + (-1)^{p-i}\left(\frac{n\Delta_q}{2\rho_q}\right)G_{7a} \tag{50}$$

$$(Z_n^{\phi\phi})_{pq} = 2j \left\{\left(\frac{k^2\Delta_p\Delta_q}{4}\right)\left(G_{5a} + \frac{\Delta_q \sin v_q}{2\rho_q} G_{5b}\right) - \left(\frac{n\Delta_q}{2\rho_q}\right)\left(\frac{n\Delta_p}{2\rho_p}\right)G_{7a}\right\} \tag{51}$$

where i is either p-1 or p and j is either q-1 or q and where

$$G_{ma} = \frac{2}{\Delta_q}\int_{\bar{t}_q}^{\bar{t}_{q+1}} G_m dt' \tag{52}$$

$$m = 5,6,7$$

$$G_{mb} = \left(\frac{2}{\Delta_q}\right)^2 \int_{\bar{t}_q}^{\bar{t}_{q+1}} (t' - t_q)G_m dt' \tag{53}$$

Equation (13) is used to rewrite (52) and (53) as

$$G_{7a} = G_{4a} + G_{5a} \tag{54}$$

$$G_{7b} = G_{4b} + G_{5b} \tag{55}$$

$$G_{ma} = \left(\frac{2}{\Delta_q}\right) \int_{\bar{t}_q}^{\bar{t}_{q+1}} G_m(t' - t_q)dt' \tag{56}$$

$$m = 4,5,6$$

$$G_{mb} = \left(\frac{2}{\Delta_q}\right)^2 \int_{\bar{t}_q}^{\bar{t}_{q+1}} (t' - t_q)G_m(t' - t_q)dt' \tag{57}$$

The argument $(t' - t_q)$ supplied with $G_m$ in (56) and (57) comes into play later on. Substitution of $R_p$ for R in (14)-(16) produces

$$G_4(t' - t_q) = 2\int_0^{\pi} d\phi \, \frac{e^{-jkR_p}}{kR_p} \sin^2\left(\frac{\phi}{2}\right) \cos(n\phi) \tag{58}$$

$$G_5(t' - t_q) = \int_0^{\pi} d\phi \, \frac{e^{-jkR_p}}{kR_p} \cos\phi \cos(n\phi) \tag{59}$$

$$G_6(t' - t_q) = \int_0^{\pi} d\phi \, \frac{e^{-jkR_p}}{kR_p} \sin\phi \sin(n\phi) \tag{60}$$

where $R_p$ is given by (32). In (32), $\rho'$ is given by (40) and $z'$ by

$$z' = z_q + (t' - t_q)\cos v_q \tag{61}$$

Equation (61) is true because the portion of the generating curve for $t_q^- < t' < t_{q+1}^-$ is straight.

Evaluation of the integrals in (56) and (57) by means of an $n_t$-point Gaussian quadrature formula gives

$$G_{ma} = \sum_{\ell'=1}^{n_t} A_{\ell'}^{(n_t)} \, G_m\!\left(\frac{1}{2}\Delta_q x_{\ell'}^{(n_t)}\right) \tag{62}$$

$$m = 4,5,6$$

$$G_{mb} = \sum_{\ell'=1}^{n_t} A_{\ell'}^{(n_t)} \, x_{\ell'}^{(n_t)} \, G_m\!\left(\frac{1}{2}\Delta_q x_{\ell'}^{(n_t)}\right) \tag{63}$$

where the abscissas $x_{\ell'}^{(n_t)}$ and weights $A_{\ell'}^{(n_t)}$ are tabulated in Appendix A of [5] for several values of $n_t$. Application of an $n_\phi$-point Gaussian quadrature formula to the integrals in (58)-(60) and replacement of $(t' - t_q)$ by $\frac{1}{2}\Delta_q x_{\ell'}^{(n_t)}$ result in

$$G_4\!\left(\frac{1}{2}\Delta_q x_{\ell'}^{(n_t)}\right) = \pi \sum_{\ell=1}^{n_\phi} A_\ell^{(n_\phi)} \frac{e^{-jkR_{p\ell'\ell}}}{kR_{p\ell'\ell}} \sin^2\!\left(\frac{\phi_\ell}{2}\right)\cos(n\phi_\ell) \tag{64}$$

$$G_5\!\left(\frac{1}{2}\Delta_q x_{\ell'}^{(n_t)}\right) = \frac{\pi}{2} \sum_{\ell=1}^{n_\phi} A_\ell^{(n_\phi)} \frac{e^{-jkR_{p\ell'\ell}}}{kR_{p\ell'\ell}} \cos\phi_\ell \cos(n\phi_\ell) \tag{65}$$

$$G_6\left(\frac{1}{2}\Delta_q\, x_{\ell'}^{(n_t)}\right) = \frac{\pi}{2}\sum_{\ell=1}^{n_\phi} A_\ell^{(n_\phi)}\, \frac{e^{-jkR_{p\ell'\ell}}}{kR_{p\ell'\ell}} \sin\phi_\ell \sin(n\phi_\ell) \tag{66}$$

where

$$R_{p\ell'\ell} = \sqrt{(\rho'-\rho_p)^2 + (z'-z_p)^2 + 4\rho_p\rho'\sin^2\left(\frac{\phi_\ell}{2}\right)} \tag{67}$$

where

$$\rho' = \rho_q + \frac{1}{2}\Delta_q\, x_{\ell'}^{(n_t)} \sin v_q \tag{68}$$

$$z' = z_q + \frac{1}{2}\Delta_q\, x_{\ell'}^{(n_t)} \cos v_q \tag{69}$$

$$\phi_\ell = \frac{\pi}{2}\left(x_\ell^{(n_\phi)} + 1\right) \tag{70}$$

Calculated values of $G_m\left(\frac{1}{2}\Delta_q\, x_{\ell'}^{(n_t)}\right)$ from (64)-(66) are substituted into (62) and (63) in order to evaluate $G_{ma}$ and $G_{mb}$. The resulting values of $G_{ma}$ and $G_{mb}$ are then substituted, either directly or through the intermediary equations (54) and (55), into formulas (48)-(51) for the elements of the moment matrix.

The values $n_t = 2$ and $n_\phi = 20$ are suggested whenever the field point is not close to the source segment. If the field point is close to the source segment, the method of eliminating the singularity [3] is used. Since double integrals are involved, three variations of the method are possible. These variations are called methods 1, 2, and 3. In method 1, elimination of the singularity is applied to the integration with respect to t'. In method 2, elimination of the singularity is applied to the integration with respect to $\phi$. In method 3, it is applied to the double integral. In methods 1 and 2, the "singular part"

of the integrand is subtracted out, numerical integration of the resulting finite integrand is performed with respect to one of the variables, the integral (with respect to this variable) of the "singular part" is added, and then numerical integration with respect to the other variable is done. In method 3, the singular part of the integrand is subtracted out, numerical integration of the resulting finite integrand is performed with respect to both variables, and then the double integral of the "singular part" is added. Method 3 is preferable to either of methods 1 and 2 because the final numerical integration in methods 1 and 2 may involve a singular integrand. However, if what is deemed to be the "singular part" can be integrated analytically with respect to only one of the variables, then either method 1 or method 2 is applicable, but method 3 is not.

Use of method 1 is now demonstrated. From (56)-(60), the required integrals with respect to t' are

$$G_a = \frac{2}{\Delta_q} \int_{\bar{t}_q}^{\bar{t}_{q+1}} \frac{e^{-jkR_p}}{kR_p} dt' \tag{71}$$

$$G_b = \left(\frac{2}{\Delta_q}\right)^2 \int_{\bar{t}_q}^{\bar{t}_{q+1}} (t' - t_q) \frac{e^{-jkR_p}}{kR_p} dt' \tag{72}$$

The above expressions are rewritten as

$$G_a = G_{a1} + G_{a2} \tag{73}$$

$$G_b = G_{b1} + G_{b2} \tag{74}$$

where

$$G_{a1} = \frac{2}{\Delta_q} \int_{\bar{t}_q}^{\bar{t}_{q+1}} \frac{e^{-jkR_p} - 1}{kR_p} dt' \tag{75}$$

$$G_{a2} = \frac{2}{\Delta_q} \int_{\bar{t}_q}^{\bar{t}_{q+1}} \frac{dt'}{kR_p} \tag{76}$$

$$G_{b1} = \left(\frac{2}{\Delta_q}\right)^2 \int_{\bar{t}_q}^{\bar{t}_{q+1}} (t' - t_q)\left(\frac{e^{-jkR_p} - 1}{kR_p}\right) dt' \tag{77}$$

$$G_{b2} = \left(\frac{2}{\Delta_q}\right)^2 \int_{\bar{t}_q}^{\bar{t}_{q+1}} \frac{(t' - t_q)dt'}{kR_p} \tag{78}$$

Application of $n_t$-point Gaussian quadrature to the right-hand sides of (75) and (77) gives

$$G_{a1} = \sum_{\ell'=1}^{n_t} A_{\ell'}^{(n_t)} G \tag{79}$$

$$G_{b1} = \sum_{\ell'=1}^{n_t} x_{\ell'}^{(n_t)} A_{\ell'}^{(n_t)} G \tag{80}$$

where

$$G = \frac{e^{-jkR_p} - 1}{kR_p} = \frac{-\sin\left(\frac{kR_p}{2}\right)\left(\sin\left(\frac{kR_p}{2}\right) + j\cos\left(\frac{kR_p}{2}\right)\right)}{\left(\frac{kR_p}{2}\right)} \tag{81}$$

where $R_p$ is to be evaluated at $(t' - t_q) = \frac{1}{2} \Delta_q x_{\ell'}^{(n_t)}$. The purpose of the alternate form of G on the extreme right-hand side of (81) is to

avoid possible roundoff error. As for the integrals in (76) and (78), we substitute (40) and (61) into (32) to obtain

$$R_p = \sqrt{(\rho_q-\rho_p+(t'-t_q)\sin v_q)^2 + (z_q-z_p+(t'-t_q)\cos v_q)^2 + + 4\rho_p(\rho_q+(t'-t_q)\sin v_q)\sin^2(\frac{\phi}{2})} \tag{82}$$

which can be rewritten as

$$R_p = \sqrt{(t'-t_q+t_o)^2 + d^2} \tag{83}$$

where

$$t_o = (\rho_q-\rho_p)\sin v_q + (z_q-z_p)\cos v_q + 2\rho_p \sin v_q \sin^2(\frac{\phi}{2}) \tag{84}$$

$$d = \sqrt{r_{pq}^2 - t_o^2} \tag{85}$$

$$r_{pq} = \sqrt{(\rho_q-\rho_p)^2 + (z_q-z_p)^2 + 4\rho_q\rho_p\sin^2(\frac{\phi}{2})} \tag{86}$$

Substitution of (83) into (76) and (78) and application of formulas 200.01 and 201.01 of Dwight [6] give

$$G_{a2} = \frac{2}{k\Delta_q} \log \tag{87}$$

$$G_{b2} = (\frac{2}{\Delta_q})^2 \frac{1}{k} [\sqrt{(t_o + \frac{\Delta_q}{2})^2 + d^2} - \sqrt{(t_o - \frac{\Delta_q}{2})^2 + d^2} - t_o \log] \tag{88}$$

where

$$\log = \begin{cases} \log\left[\dfrac{|t_o| + \frac{\Delta_q}{2} + \sqrt{(|t_o| + \frac{\Delta_q}{2})^2 + d^2}}{|t_o| - \frac{\Delta_q}{2} + \sqrt{(|t_o| - \frac{\Delta_q}{2})^2 + d^2}}\right], & |t_o| \geq \dfrac{\Delta_q}{2} \\ \log\left[\dfrac{\left[|t_o| + \frac{\Delta_q}{2} + \sqrt{(|t_o| + \frac{\Delta_q}{2})^2 + d^2}\right]\left[\frac{\Delta_q}{2} - |t_o| + \sqrt{(\frac{\Delta_q}{2} - |t_o|)^2 + d^2}\right]}{d^2}\right], & |t_o| < \dfrac{q}{2} \end{cases} \tag{89}$$

To reduce roundoff error, (88) is rewritten as

$$G_{b2} = \left(\frac{2}{\Delta_q}\right)\frac{t_o}{k}\left[\frac{4}{\sqrt{(t_o + \frac{\Delta_q}{2})^2 + d^2} + \sqrt{(t_o - \frac{\Delta_q}{2})^2 + d^2}} - \frac{2}{\Delta_q}\log\right] \tag{90}$$

The calculated values of $G_a$ are used to obtain $G_{ma}$ according to

$$G_{4a} = \pi \sum_{\ell=1}^{n_\phi} G_a A_\ell^{(n_\phi)} \sin^2\left(\frac{\phi_\ell}{2}\right)\cos(n\phi_\ell) \tag{91}$$

$$G_{5a} = \frac{\pi}{2} \sum_{\ell=1}^{n_\phi} G_a A_\ell^{(n_\phi)} \cos\phi_\ell \cos(n\phi_\ell) \tag{92}$$

$$G_{6a} = \frac{\pi}{2} \sum_{\ell=1}^{n_\phi} G_a A_\ell^{(n_\phi)} \sin\phi_\ell \sin(n\phi_\ell) \tag{93}$$

where $G_a$ is to be evaluated at $\phi = \phi_\ell$ given by (70). Equations (91)-(93) are also valid with a replaced by b. Calculation of $G_a$ and $G_b$ should be according to the development (73)-(90) only for those values of $\phi_\ell$ for which $r_{pq}$ is either smaller than or comparable to $\Delta_q$. If $r_{pq}$ is considerably larger than $\Delta_q$, pure Gaussian quadrature is adequate.

Use of method 2 is now demonstrated. Since the integrands of (58) and (60) are fairly well-behaved, method 2 is applied only to (59).

In method 2, $G_{5a}$ and $G_{5b}$ are calculated according to (62) and (63) with $G_5(\frac{1}{2}\,\Delta_q\, x_{\ell'}^{(n_t)})$ given not by (65) but by

$$G_5(\tfrac{1}{2}\,\Delta_q x_{\ell'}^{(n_t)}) = \frac{\pi}{2}\sum_{\ell=1}^{n_\phi} A_\ell^{(n_\phi)} \frac{e^{-jkR_{p\ell'\ell}}}{kR_{p\ell'\ell}} \cos\phi_\ell \cos(n\phi_\ell) -$$

$$-\frac{\pi}{2}\sum_{\ell=1}^{n_\phi} \frac{A_\ell^{(n_\phi)}}{k\sqrt{(\rho'-\rho_p)^2 + (z'-z_p)^2 + \rho'\rho_p\phi^2}}$$

$$+\int_{\phi=0}^{\pi} \frac{d\phi}{k\sqrt{(\rho'-\rho_p)^2 + (z'-z_p)^2 + \rho'\rho_p\phi^2}} \tag{94}$$

From formula 200.01. of Dwight [6],

$$\int_{\phi=0}^{\pi} \frac{d\phi}{k\sqrt{(\rho'-\rho_p)^2+(z'-z_p)^2 + \rho'\rho_p\phi^2}} = \frac{1}{k\sqrt{\rho'\rho_p}} \log\,(u + \sqrt{1+u^2}) \tag{95}$$

where

$$u = \frac{\pi\sqrt{\rho'\rho_p}}{\sqrt{(\rho'-\rho_p)^2 + (z'-z_p)^2}} \tag{96}$$

Equation (94) should be used only for those values of t' for which $\rho_q$ is considerably larger than $\sqrt{(\rho'-\rho_p)^2 + (z'-z_p)^2}$. Otherwise, the pure Gaussian quadrature of (65) is adequate.

Use of method 3 is now demonstrated for the case in which p=q. Method 3 is applied only to the calculation of $G_{5a}$ because $G_{5a}$ is the only integral in (56) and (57) whose integrand is not bounded. We write

$$G_{5a} = \frac{\pi}{2} \sum_{\ell=1}^{n_\phi} A_\ell^{(n_\phi)} \cos\phi_\ell \cos(n\phi_\ell) \sum_{\ell'=1}^{n_t} A_{\ell'}^{(n_t)} \frac{e^{-jkR_{p\ell'\ell}}}{kR_{p\ell'\ell}} -$$

$$- \frac{\pi}{2} \sum_{\ell=1}^{n_\phi} A_\ell^{(n_\phi)} \sum_{\ell'=1}^{n_t} \frac{A_{\ell'}^{(n_t)}}{k\sqrt{\left(\frac{\Delta_q}{2} x_{\ell'}^{(n_t)}\right)^2 + \rho_q^2\phi_\ell^2}} + \frac{2}{\Delta_q}\int_0^\pi d\phi \int_{t_q^-}^{t_{q+1}^-} \frac{dt'}{k\sqrt{(t'-t_q)^2+\rho_q^2\phi^2}} \tag{97}$$

Because of the formula

$$\frac{d^2}{dxdy}\left[x \log(y + \sqrt{x^2+y^2}) + y \log(x + \sqrt{x^2+y^2})\right] = \frac{1}{\sqrt{x^2+y^2}} \quad , \tag{98}$$

the double integral in (97) is tractable.

$$\frac{2}{\Delta_q}\int_0^\pi d\phi \int_{t_q^-}^{t_{q+1}^-} \frac{dt'}{k\sqrt{(t'-t_q)^2 + \rho_q^2\phi^2}} = \frac{2}{k\rho_q}\left[\log\left[\frac{2\pi\rho_q}{\Delta_q} + \sqrt{1 + \left(\frac{2\pi\rho_q}{\Delta_q}\right)^2}\right] + \right.$$

$$\left. + \frac{2\pi\rho_q}{\Delta_q} \log\left[\frac{\Delta_q}{2\pi\rho_q} + \sqrt{1 + \left(\frac{\Delta_q}{2\pi\rho_q}\right)^2}\right]\right] \tag{99}$$

In each of methods 1, 2, and 3, an attempt is made to subtract out the singularity due to $1/R_p$ in (58)-(60). In method 1, $1/R_p$ itself is subtracted out. In method 2, the approximation

$$\frac{1}{\sqrt{(\rho'-\rho_p)^2 + (z'-z_p)^2 + \rho_p\rho'\phi^2}}$$

to $1/R_p$ is subtracted out. For comparison, $R_p$ is given by (32). In method 3, the approximation

$$\frac{1}{\sqrt{(\rho'-\rho_p)^2 + (z'-z_p)^2 + \rho_p\rho_q\phi^2}}$$

to $1/R_p$ is subtracted out for p=q. Because the double integral of this approximation is tractable, method 3 can be extended to cover the case in which $p \neq q$. For $p \neq q$, the alternate approximation

$$\frac{1}{\sqrt{(\rho'-\rho_p)^2 + (z'-z_p)^2 + \rho_p \rho_{min} \phi^2}}$$

to $1/R_p$ merits consideration. Here, $\rho_{min}$ is the value of $\rho'$ at that value of t' which minimizes $(\rho'-\rho_p)^2 + (z'-z_p)^2$. No matter which of the above two approximations to $1/R_p$ is used, the closed form expression for its double integral is rather complicated and vulnerable to roundoff error. For this reason, method 3 was used only for p=q.

For $p \neq q$, the decision whether to use methods 1 or 2 is based on comparisons of $\Delta_q$ with $d_o$ and $\rho_q$ with $d_o$ where $d_o$ is the distance from the field point at $t = t_p$ to the nearest point on the qth source segment. The distance between the field point at $t = t_p$ and the point $(t',\phi)$ on the qth source segment is given by (82) or (83). It is evident that the minimum of (82) occurs at $\phi = 0$ because neither $\rho_p$ nor $\rho'$ of (40) can be negative. At $\phi = 0$, (84) and (85) specialize to

$$t_o^* = (\rho_q - \rho_p) \sin v_q + (z_q - z_p) \cos v_q \tag{100}$$

$$d^* = |(\rho_q - \rho_p) \cos v_q - (z_q - z_p) \sin v_q| \tag{101}$$

The asterisk ($^*$) on the left-hand sides of (100) and (101) indicates that $\phi = 0$. Minimizing (83) with respect to t' on the qth source segment where $-\frac{\Delta_q}{2} \leq t' - t_q \leq \frac{\Delta_q}{2}$, we obtain

$$d_o = \begin{cases} d^* & |t_o^*| \le \frac{\Delta_q}{2} \\ \sqrt{(|t_o^*| - \frac{\Delta_q}{2})^2 + (d^*)^2} & |t_o^*| > \frac{\Delta_q}{2} \end{cases} \tag{102}$$

If

$$\left.\begin{array}{r} p \neq q \\ \frac{1}{2} c_t \Delta_q \le d_o \\ c_\phi \rho_q \le d_o \end{array}\right\} \quad \begin{array}{c} \text{Case 1} \\ \text{Pure quadrature} \end{array} \tag{103}$$

then the pure quadrature of (62) - (66) is used to calculate $G_{ma}$ and $G_{mb}$. Here, $c_t$ and $c_\phi$ are constants for which the values

$$\begin{aligned} c_t &= 2. \\ c_\phi &= 0.1 \end{aligned} \tag{104}$$

are suggested. If

$$\left.\begin{array}{r} p \neq q \\ \frac{1}{2} c_t \Delta_q > d_o \\ c_\phi \rho_q \le d_o \end{array}\right\} \quad \begin{array}{c} \text{Case 2} \\ \text{Method 1} \end{array} \tag{105}$$

then method 1 is used. If

$$\left.\begin{array}{r} p \neq q \\ c_\phi \rho_q > d_o \end{array}\right\} \quad \begin{array}{c} \text{Case 3} \\ \text{Method 2} \end{array} \tag{106}$$

then method 2 is used. If

$$p = q \; \Big\} \quad \begin{array}{c} \text{Case 4} \\ \text{Methods 1 and 3} \end{array} \tag{107}$$

then both methods 1 and 3 are used.

The strategy in (103) and (105)-(107) is based on the assumptions that the Gaussian quadrature integration with respect to $t'$ must be fortified only when $\Delta_q$ is large, and that the Gaussian quadrature integration with respect to $\phi$ must be fortified only when $\rho_q$ is large. The integration with respect to $t'$ could not be fortified for $\frac{1}{2} c_t \Delta_q > d_o$ in Case 3 because methods 1 and 2 can not be applied simultaneously and because it was decided earlier to limit use of method 3 to Case 4. However, pure Gaussian quadrature should still give a fairly accurate evaluation of this integral with respect to $t'$ because of the following reasoning. Since $\rho'$ is large, difficulty can only occur when $\phi$ is small. Furthermore, this difficulty is not usually serious because $\Delta_q \leq 2d_o$ most often. It is evident that $\Delta_q \leq 2d_o$ if $p \neq q$, if all the $\Delta_q$ are equal, and if the generating curve does not fold back on itself.

## IV. EVALUATION OF THE PLANE WAVE EXCITATION VECTOR

Consider the elements (7) and (8) of the excitation vector for a $\theta$-polarized incident plane wave defined by

$$\underline{E}^i = u_\theta^t k\eta \, \underline{e}^{-j\underline{k}_t \cdot \underline{r}} \tag{108}$$

and also for a $\phi$-polarized incident plane wave defined by

$$\underline{E}^i = \underline{u}_\phi^t k\eta \, e^{-j\underline{k}_t \cdot \underline{r}} \tag{109}$$

In (108) and (109),

$$\underline{k}_t = - k(\underline{u}_x \sin \theta_t + \underline{u}_z \cos \theta_t) \tag{110}$$

$$\underline{u}_\theta^t = \underline{u}_x \cos \theta_t - \underline{u}_z \sin \theta_t \tag{111}$$

$$\underline{u}_\phi^t = \underline{u}_y \tag{112}$$

where $\theta_t$ is the angle of incidence and where $\underline{u}_x$, $\underline{u}_y$, and $\underline{u}_z$ are unit vectors in the x,y, and z directions, respectively. Also, $\underline{r}$ is the radius vector from the origin. The origin must lie on the axis of the body of revolution because this axis is the z axis. Substitution of (4), (5), and (108) into (7) and (8) gives

$$V_{ni}^{t\theta} = j^n \pi k \int_{\bar{t}_i}^{\bar{t}_{i+2}} dt \; T_i(t)\{j \sin v \cos \theta_t (J_{n+1} - J_{n-1}) - 2 \cos v \sin \theta_t J_n\} e^{jkz \cos \theta_t} \tag{113}$$

$$V_{ni}^{\phi\theta} = j^n \pi k \int_{\bar{t}_i}^{\bar{t}_{i+1}} dt \; \frac{\rho}{\rho_i} P_i(t) \; (J_{n+1} + J_{n-1}) \cos \theta_t \; e^{jkz \cos \theta_t} \tag{114}$$

where $V_{ni}^{t\theta}$ is $V_{ni}^t$ for $\underline{E}^i$ given by (108) and $V_{ni}^{\phi\theta}$ is $V_{ni}^\phi$ for $\underline{E}^i$ given by (108). In (113) and (114),

$$J_n = J_n(k\rho \sin \theta_t) \tag{115}$$

where $J_n$ is the Bessel function of the first kind. Likewise, substitution of (4), (5), and (109) into (7) and (8) gives

$$V_{ni}^{t\phi} = - j^n \pi k \int_{t_i^-}^{t_{i+2}^-} dt\ T_i(t)(J_{n+1} + J_{n-1}) \sin v\ e^{jkz \cos \theta_t} \tag{116}$$

$$V_{ni}^{\phi\phi} = j^{n+1} \pi k \int_{t_i^-}^{t_{i+1}^-} dt\ \frac{\rho}{\rho_i} P_i(t)\ (J_{n+1} - J_{n-1}) e^{jkz \cos \theta_t} \tag{117}$$

where the second superscript on V on the left-hand sides of (116) and (117) denotes excitation by the $\phi$-polarized incident plane wave (109). The manipulations required to obtain (113)-(117) are similar to those used in the derivation of (1-95).

The contributions to (113) and (116) due to integration with respect to t from $t_p^-$ to $t_{p+1}^-$ are expressed by

$$\overset{*}{V}{}_{ni}^{t\theta} = j^n \pi k \int_{t_p^-}^{t_{p+1}^-} dt\ T_i(t)\{j \sin v \cos \theta_t (J_{n+1} - J_{n-1}) - 2 \cos v \sin \theta_t J_n\} e^{jkz \cos \theta_t} \tag{118}$$

$$\overset{*}{V}{}_{ni}^{t\phi} = - j^n \pi k \int_{t_p^-}^{t_{p+1}^-} dt\ T_i(t)(J_{n+1} + J_{n-1}) \sin v\ e^{jkz \cos \theta_t} \tag{119}$$

where i is either p-1 or p. The asterisk ($^*$) on the left-hand sides of (118) and (119) denotes the contribution due to integration from $t_p^-$ to $t_{p+1}^-$. First, v is replaced by $v_p$ in (118) and (119). Throughout (114), (117), (118), and (119), $P_i(t)$, $T_i(t)$, and $\rho$ are expressed according to

(36), (37), and (40), respectively. Then, i is replaced by p in (114) and (117) to make those equations compatible with (118) and (119). The results of the above substitutions are

$$\overset{*}{V}{}^{t\theta}_{ni} = \frac{j^n\pi k}{2}\int_{\bar{t}_p}^{\bar{t}_{p+1}} dt\ \left(1 + \frac{(-1)^{p-i}2(t-t_p)}{\Delta_p}\right)\{j\ \sin v_p \cos\theta_t (J_{n+1}-J_{n-1}) - -2\cos v_p \sin\theta_t J_n\}\ e^{jkz\cos\theta_t} \tag{120}$$

$$V^{\phi\theta}_{np} = j^n\pi k \int_{\bar{t}_p}^{\bar{t}_{p+1}} dt\ \left(1 + \frac{(t-t_p)\sin v_p}{\rho_p}\right)(J_{n+1}+J_{n-1})\cos\theta_t\ e^{jkz\cos\theta_t} \tag{121}$$

$$\overset{*}{V}{}^{t\phi}_{ni} = -\frac{j^n\pi k}{2}\int_{\bar{t}_p}^{\bar{t}_{p+1}} dt\left(1 + \frac{(-1)^{p-i}2(t-t_p)}{\Delta_p}\right)(J_{n+1}+J_{n-1})\sin v_p\ e^{jkz\cos\theta_t} \tag{122}$$

$$V^{\phi\phi}_{np} = j^{n+1}\pi k \int_{\bar{t}_p}^{\bar{t}_{p+1}} dt\ \left(1 + \frac{(t-t_p)\sin v_p}{\rho_p}\right)(J_{n+1}-J_{n-1})\ e^{jkz\cos\theta_t} \tag{123}$$

where i is either p-1 or p in (120) and (122).

Equations (120)-(123) can be rewritten as

$$\overset{*}{V}{}^{t\theta}_{ni} = \frac{j^{n+1}\ \pi k\Delta_p \sin v_p \cos\theta_t}{4}(F_{n+1,a}-F_{n-1,a}) - \frac{j^n\pi k\Delta_p \cos v_p \sin\theta_t}{2}F_{na} + +(-1)^{p-i}\left\{\frac{j^{n+1}\pi k\Delta_p \sin v_p \cos\theta_t}{4}(F_{n+1,b}-F_{n-1,b}) - \frac{j^n\pi k\Delta_p \cos v_p \sin\theta_t}{2}F_{nb}\right\} \tag{124}$$

$$V^{\phi\theta}_{np} = \frac{j^n\pi k\Delta_p \cos\theta_t}{2}\left\{(F_{n+1,a}+F_{n-1,a}) + \frac{\Delta_p \sin v_p}{2\rho_p}(F_{n+1,b}+F_{n-1,b})\right\} \tag{125}$$

$$\overset{*}{V}{}^{t\phi}_{ni} = -\frac{j^n \pi k \Delta_p \sin v_p}{4} (F_{n+1,a}+F_{n-1,a}) - \frac{(-1)^{p-i} j^n \pi k \Delta_p \sin v_p}{4} (F_{n+1,b}+F_{n-1,b}) \tag{126}$$

$$V^{\phi\phi}_{np} = \frac{j^{n+1} \pi k \Delta_p}{2} \{(F_{n+1,a}-F_{n-1,a}) + \frac{\Delta_p \sin v_p}{2\rho_p} (F_{n+1,b}-F_{n-1,b})\} \tag{127}$$

where i is either p-1 or p in (124) and (126). In (124)-127),

$$F_{ma} = \frac{2}{\Delta_p} \int_{\bar{t}_p}^{\bar{t}_{p+1}} J_m(k\rho \sin \theta_t) e^{jkz \cos \theta_t} dt \tag{128}$$

$$m=n-1,n,n+1$$

$$F_{mb} = (\frac{2}{\Delta_p})^2 \int_{\bar{t}_p}^{\bar{t}_{p+1}} (t-t_p) J_m(k\rho \sin \theta_t) e^{jkz \cos \theta_t} dt \tag{129}$$

where, from (40) and (61),

$$\rho = \rho_p + (t-t_p) \sin v_p \tag{130}$$

$$z = z_p + (t-t_p) \cos v_p \tag{131}$$

Evaluation of (128) and (129) by means of an $n_T$-point Gaussian quadrature formula yields

$$\left.\begin{aligned} F_{ma} &= \sum_{\ell=1}^{n_T} A_\ell^{(n_T)} J_m(k\hat{\rho}_\ell \sin \theta_t) e^{jk\hat{z}_\ell \cos \theta_t} && (132) \\ F_{mb} &= \sum_{\ell=1}^{n_T} A_\ell^{(n_T)} x_\ell^{(n_T)} J_m(k\hat{\rho}_\ell \sin \theta_t) e^{jk\hat{z}_\ell \cos \theta_t} && (133) \end{aligned}\right\} m=n-1,n,n+1$$

where

$$\hat{\rho}_\ell = \rho_p + \frac{\Delta_p x_\ell^{(n_T)}}{2} \sin v_p \tag{134}$$

$$\hat{z}_\ell = z_p + \frac{\Delta_p x_\ell^{(n_T)}}{2} \cos v_p \tag{135}$$

The calculation of the plane wave excitation vector would be most nearly consistent with the calculation of the moment matrix if $n_T = 1$. For $n_T = 1$, the extra data $x_1^{(1)} = 0$ and $A_1^{(1)} = 2$ must be supplied. Now, assuming that $n_t > 1$, it could be said that $n_t$-point quadrature is more accurate than 1-point quadrature. The $n_t$-point quadrature data are already available because they were used to calculate tne elements of the moment matrix in Section III. With $n_t$ fixed at 2, results were calculated for both $n_T = 1$ and $n_T = 2$. It was difficult to tell which results were more accurate. The numerical results presented in Section V were obtained by using $n_t = n_T = 2$.

## V. NUMERICAL RESULTS

Computer program subroutines have been written to calculate the elements of the moment matrix and the elements of the plane wave excitation vector. These subroutines are described and listed in Part Two of this report. They were used to calculate the electric currents induced by a plane wave axially incident on two circular disks, a thin washer, a cone-sphere, an open cylinder, and a spherical shell with an axially symmetric aperture. The magnitudes of these electric currents are plotted in this section.

For axial incidence, $\theta_t$ is either 0° or 180° and the only non-zero excitation vectors for the θ-polarized plane wave (108) are

$$\begin{bmatrix} \vec{V}^t_{-1} \\ \\ \vec{V}^\phi_{-1} \end{bmatrix} = \begin{bmatrix} \vec{V}^t_1 \\ \\ -\vec{V}^\phi_1 \end{bmatrix} \tag{136}$$

It is evident from (9)-(17) that

$$\begin{bmatrix} Z^{tt}_{-1} & Z^{t\phi}_{-1} \\ \\ Z^{\phi t}_{-1} & Z^{\phi\phi}_{-1} \end{bmatrix} = \begin{bmatrix} Z^{tt}_1 & -Z^{t\phi}_1 \\ \\ -Z^{\phi t}_1 & Z^{\phi\phi}_1 \end{bmatrix} \tag{137}$$

In consequence of (136), (137), and (6), the only non-zero column vectors $\vec{I}^t_n$ and $\vec{I}^\phi_n$ are given by

$$\begin{bmatrix} \vec{I}^t_{-1} \\ \\ \vec{I}^\phi_{-1} \end{bmatrix} = \begin{bmatrix} \vec{I}^t_1 \\ \\ -\vec{I}^\phi_1 \end{bmatrix} \tag{138}$$

where the column vector on the right-hand side of (138) satisfies (6) for n=1.

In view of (2) and (3), substitution of (138) into (1) and subsequent division by k give

$$\frac{\underline{J}}{|\underline{H}^i|} = 2\underline{u}_t \cos\phi \left(\sum_j I^t_{1j} \frac{T_j(t)}{k\rho}\right) + 2j\,\underline{u}_\phi \sin\phi \left(\sum_j I^\phi_{1j} \frac{P_j(t)}{k\rho_j}\right) \tag{139}$$

The $|\underline{H}^i|$ written instead of k on the left-hand side of (139) is the magnitude of the incident magnetic field associated with (108). This $|\underline{H}^i|$ is indeed equal to k. At $t = t^-_{p+1}$, the t component of (139) reduces to

$$\frac{J_t}{|\underline{H}^i|} = \frac{2I^t_{1p}}{k\rho(t^-_{p+1})} \cos\phi \;, \quad p=1,2,\ldots P-2 \tag{140}$$

At $t = t_p$, the $\phi$ component of (139) reduces to

$$\frac{J_\phi}{|\underline{H}^i|} = \frac{2jI^\phi_{1p}}{k\rho_p} \sin\phi \quad, \qquad p=1,2,\ldots P-1 \tag{141}$$

Here, $J_t$ and $J_\phi$ are, respectively, the t and $\phi$ components of $\underline{J}$. In the figures to follow, $\frac{|J_t|}{|\underline{H}^i|}$ in the $\phi$ = 0° plane is plotted with squares and $\frac{|J_\phi|}{|\underline{H}^i|}$ in the $\phi$ = 90° plane is plotted with octagons.

Figure 4 shows the t and $\phi$ components $\frac{|J_t|}{|\underline{H}^i|}$ and $\frac{|J_\phi|}{|\underline{H}^i|}$ of the electric current induced by the axially incident electric field (108) with $\theta_t = 0$ on an infinitely thin circular disk of radius 0.25λ where λ is the wavelength. In Fig. 4, $\frac{|J_t|}{|\underline{H}^i|}$ is plotted with squares and $\frac{|J_\phi|}{|\underline{H}^i|}$ with octagons.

Both quantities are plotted versus $t/\lambda$ where t is the arc length along the generating curve. The horizontal axis in Fig. 4 was labeled $T/\lambda$ because the lower case letter t could not be drawn by the plotter. In Fig. 4, the center of the disk is at $t = 0$ and the edge at $t = 0.25\lambda$. The electric currents in Fig. 4 and in Figs. 5-10 to follow were calculated with $n_t = n_T = 2$, $n_\phi = 20$ and with the points $\bar{t}_j$, $j=1,2,\ldots P$ equally spaced along the generating curve. Since 12 octagons are in Fig. 4, P=13 therein. The electric current in Fig. 4 should be twice as large as the magnetic current in Fig. 4 on page 32 of [7].

Figure 5 shows the electric current induced on a circular disk of radius $1.5\lambda$ by the same axially incident plane wave as in Fig. 4. The electric current in Fig. 5 should be twice as large as the magnetic current in Fig. 6 on page 33 of [7]. Figure 6 shows the electric current for axial incidence on an infinitely thin washer of inner radius $0.4\lambda$ and outer radius $1.2\lambda$. The inner edge of the washer is at $t = 0$ and the outer edge at $t = 0.8\lambda$. Figure 6 should be compared with Fig. 3 of [8]. The size of the washer in Fig. 3 of [8] is incorrectly stated. That figure is actually a plot of the electric current on the same washer as in Fig. 6.

Figures 7 and 8 are plots of the electric current for axial incidence on a cone-sphere of cone angle 20° and sphere radius $0.2\lambda$. Figure 7 is for incidence on the sphere end and Fig. 8 is for incidence on the tip of the cone. The tip of the cone is at $t = 0$. At the sphere end, t is approximately $1.48\lambda$. For comparison, see Fig. 4.15 on page 218 of [9].

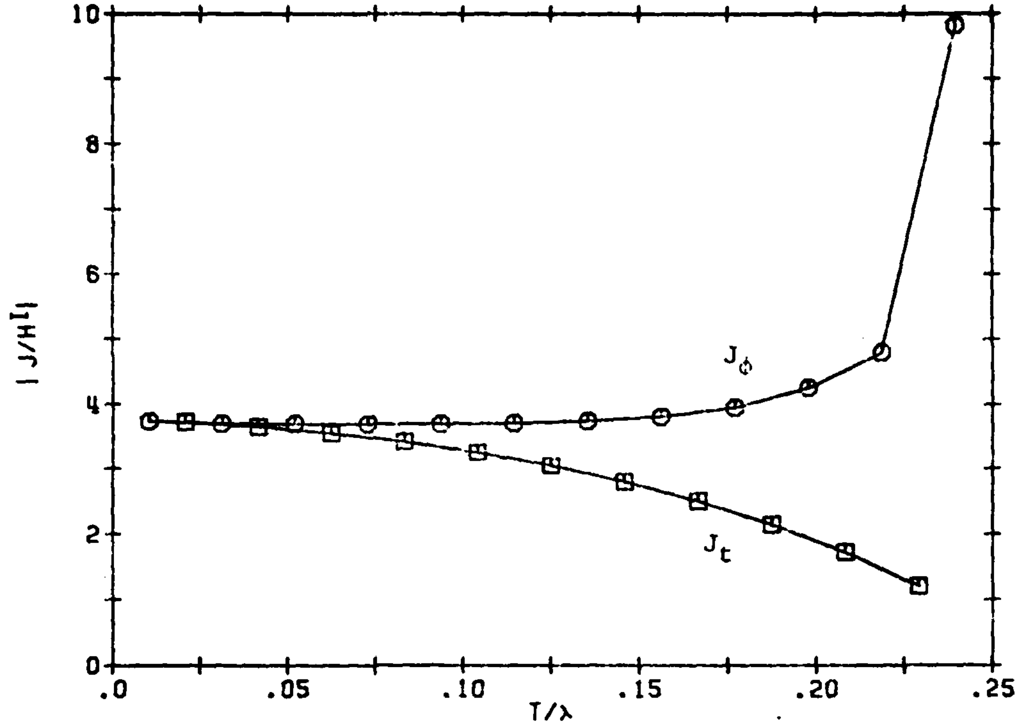


Fig. 4. Electric current for axial incidence on a circular disk of radius 0.25λ, t = 0 at center.

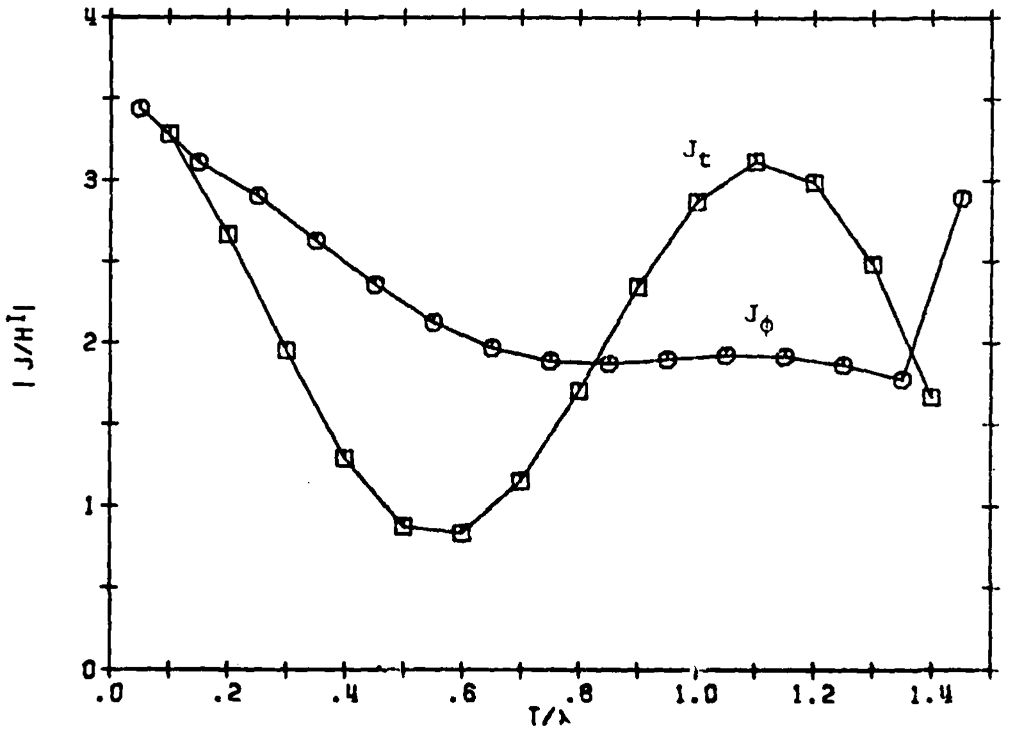


Fig. 5. Electric current for axial incidence on a circular disk of radius 1.5λ, t = 0 at center.

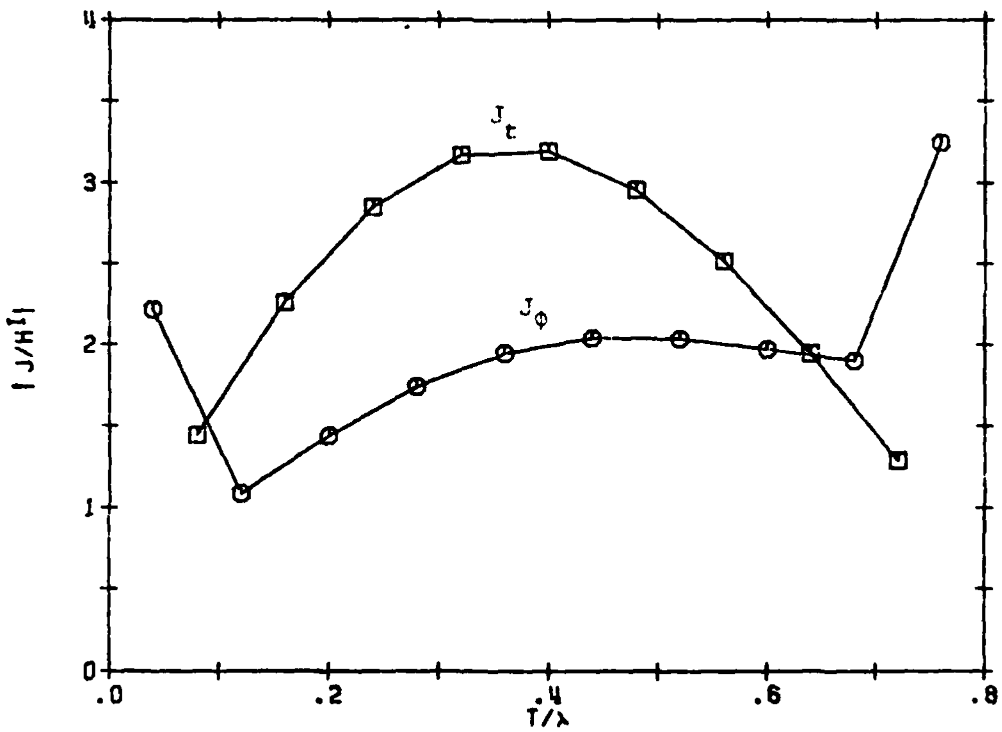


Fig. 6. Electric current for axial incidence on a circular washer of inside radius 0.4λ and outside radius 1.2λ, t = 0 at inside edge.

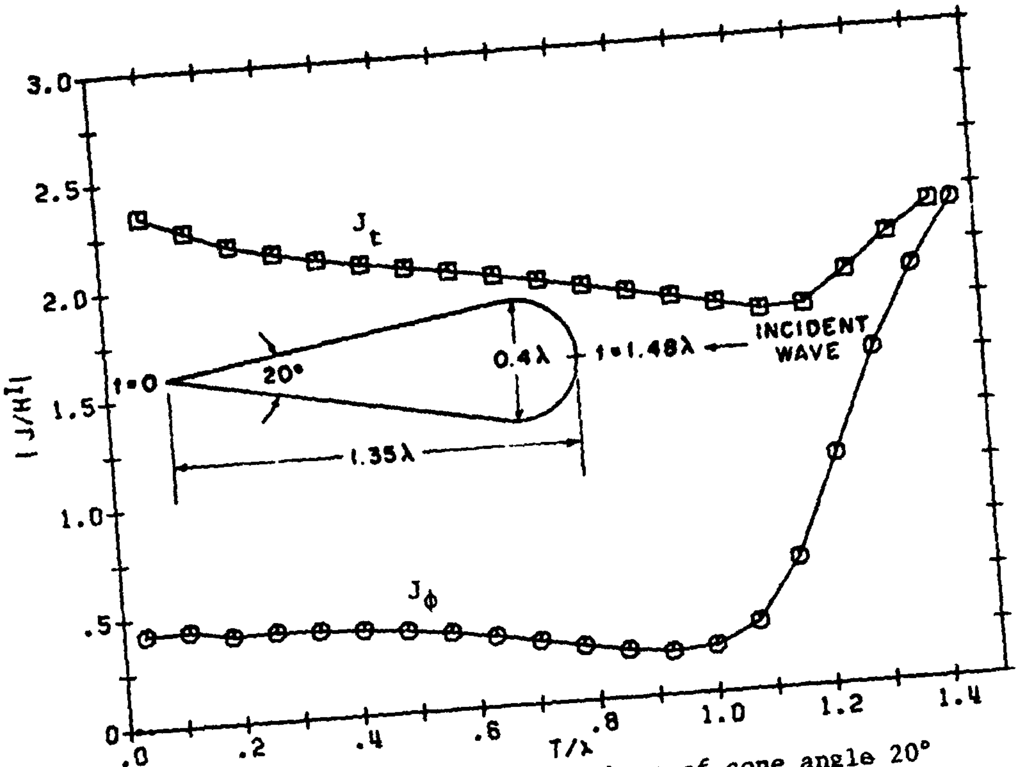


Fig. 7. Electric current on a cone-sphere of cone angle 20° and sphere radius 0.2λ, incidence on sphere.

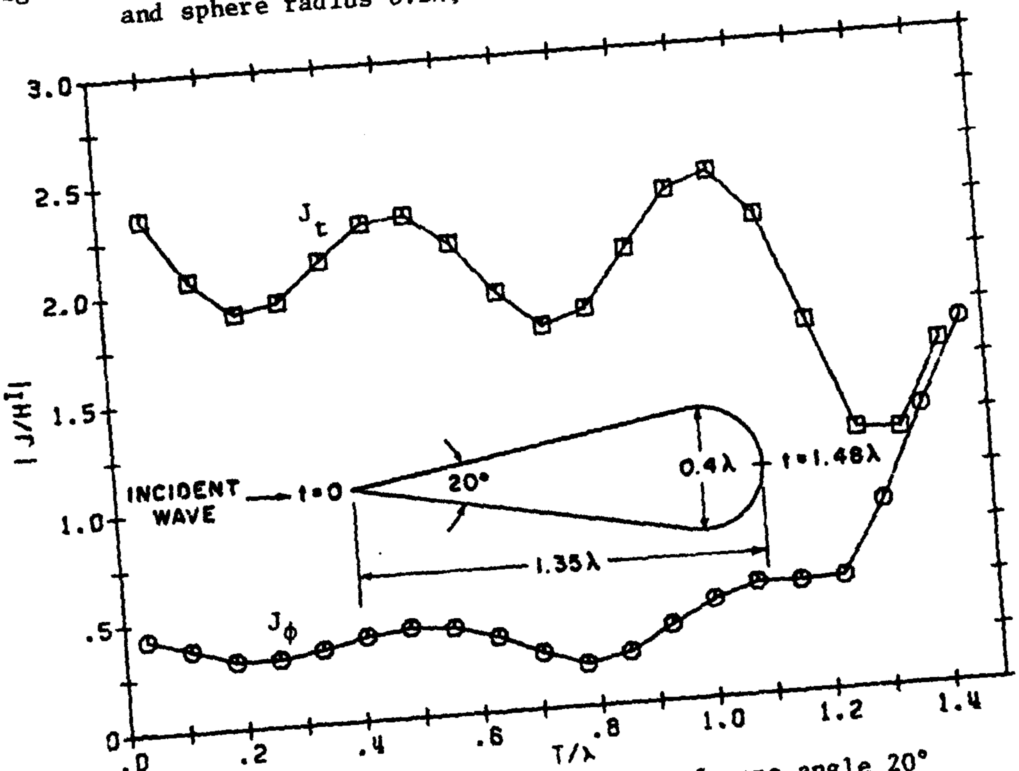


Fig. 8. Electric current on a cone-sphere of cone angle 20° and sphere radius 0.2λ, incidence on tip.

Figure 9 shows the electric current for axial incidence on an open-ended cylinder of radius $\lambda/2\pi$ and length $\lambda$. The plane wave is incident on the end of the cylinder for which $t = 0$. The excellent results plotted in Fig. 9 here and in Fig. 2.13 on page 52 of [2] were both obtained by using the electric field integral equation, notwithstanding the stability problem reported in [10].

Figure 10 is a plot of the electric current for axial incidence on the infinitely thin conducting shell for which

$$r = 0.2\lambda$$
$$45° \leq \theta \leq 180°$$

where $r$ and $\theta$, being spherical coordinates, are the radius and colatitude, respectively. This shell is a spherical shell with an axially symmetric aperture. The pole of the shell is at $t = 0$. At the edge of the shell, $t$ is approximately $0.471\lambda$. The plane wave is incident on the aperture.

Numerical results for the electric current on a circular disk of radius $0.02\lambda$ not shown here exhibited a noticeable change in slope near the center of the disk. The curves labeled "a" in Figs. 7 and 8 on page 34 of [7] also indicate a change in the slope of the magnetic current near the center of the complementary aperture. However, these changes in slope did not agree with each other. Now, equation (23) of [11] does not predict any noticeable change in the slope of the electric current near the center of the disk of radius $0.02\lambda$. The changes in slope obtained by using the computer program of the present

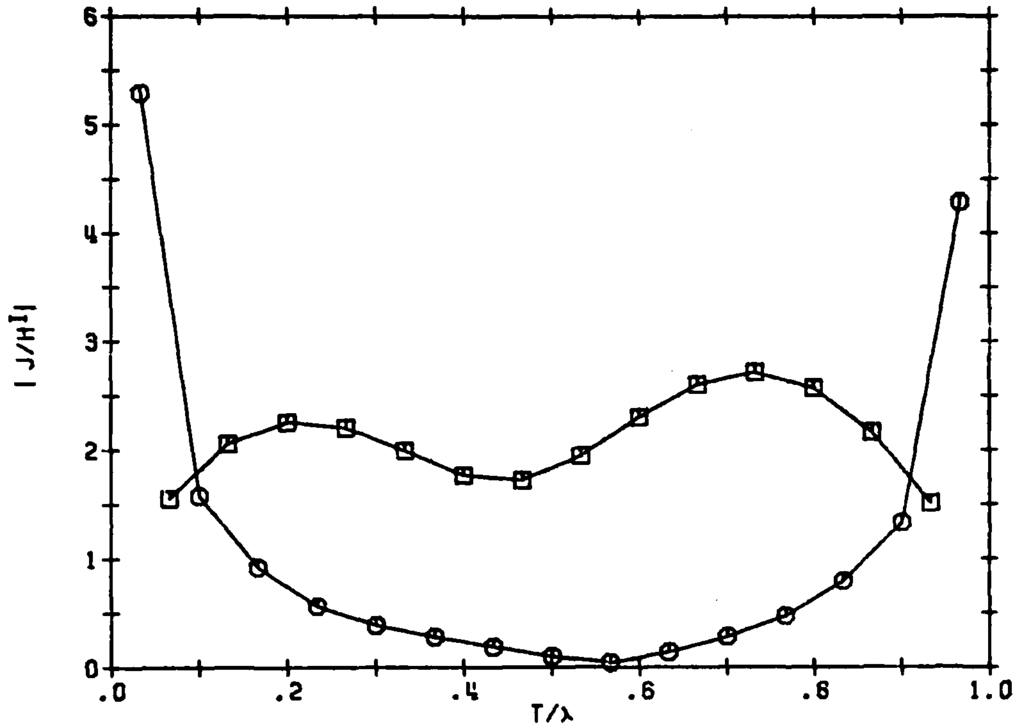


Fig. 9. Electric current on an open-ended cylinder of radius $\lambda/(2\pi)$ and length $\lambda$, incidence on $t = 0$.

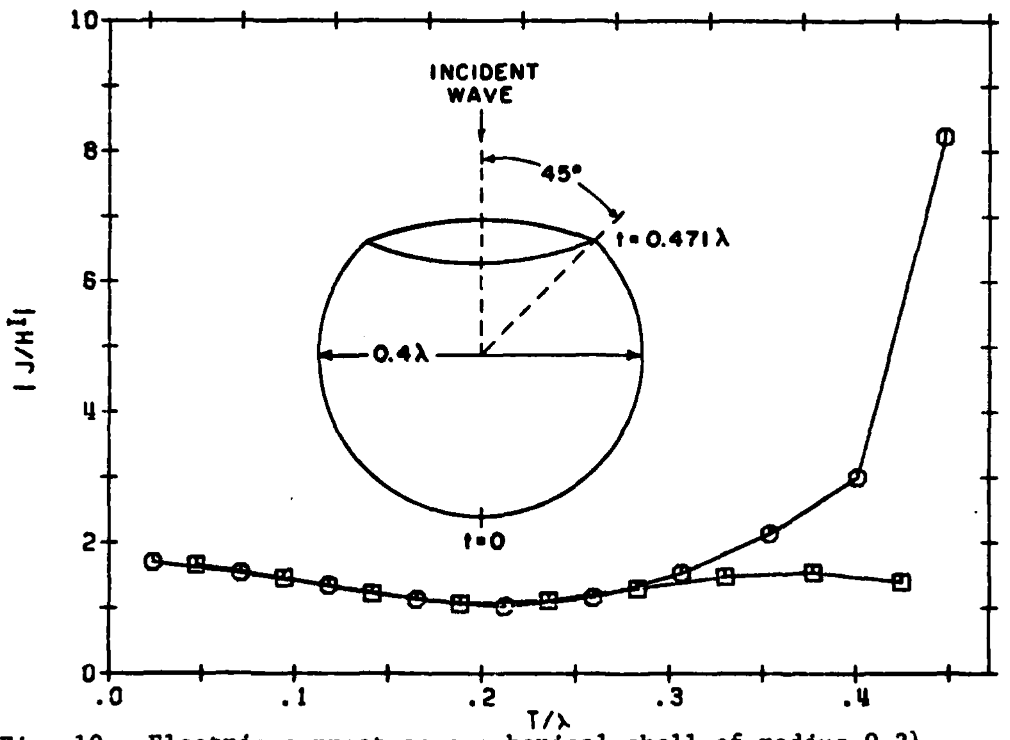


Fig. 10. Electric current on a spherical shell of radius $0.2\lambda$ with axially symmetric aperture, edge at $t = 0.471\lambda$, incidence on aperture.

report and the program of [7] are obviously wrong. The changes in slope obtained by using these programs are much more pronounced for the disk of radius 0.002λ. However, they disappear when all calculations are done in double precision. Hence, these changes in slope are due to severe roundoff error. This roundoff error occurs because the vector potential terms, those containing the factor $k^2$ explicit in (9)-(12), are overshadowed by the rest of the terms in (9)-(12), the scalar potential terms. If these vector potential terms were set equal to zero, the moment matrix would be singular because there are several linear combinations of the expansion functions which have no electric charge associated with them.

PART TWO

COMPUTER PROGRAM

## I. INTRODUCTION

The computer program which implements the numerical solution expounded in Part One is described and listed here in Part Two. This program consists of the subroutine ZMAT, the function BLOG, the subroutines PLANE, DECOMP, and SOLVE, and a main program. The subroutine ZMAT calculates the elements of the moment matrix in (6). The function BLOG is called by ZMAT. The subroutine PLANE calculates the elements of the excitation vector in (6) for plane wave incidence. The subroutines DECOMP and SOLVE solve the matrix equation (6) for $\vec{I}_n^t$ and $\vec{I}_n^\phi$.

The main program obtains the electric current induced on the surface of the body of revolution by the axially incident plane wave (108) with $\theta_t = 0$ or $\pi$ radians. The main program calls the subroutines ZMAT, PLANE, DECOMP, and SOLVE. It is not difficult to generalize the main program to oblique incidence because the subroutines ZMAT, PLANE, DECOMP, and SOLVE are designed to calculate $\vec{I}_n^t$ and $\vec{I}_n^\phi$ for $n = 0,1,2,\ldots$, For the $\theta$-polarized incident plane wave (108), $\vec{I}_n^t$ is even in n and $\vec{I}_n^\phi$ is odd in n. For the $\phi$ polarization (109), $\vec{I}_n^t$ is odd in n and $\vec{I}_n^\phi$ is even in n. In order to obtain far field patterns, the main program must be supplied with additional logic. This additional logic is outlined as follows. According to (1-91), the far field is obtained by premultiplying the solution vector to (6) by plane wave measurement matrices for $n = 0, \pm 1, \pm 2, \ldots$ . The plane wave measurement matrices for $n = 0,1,2,\ldots$

can be obtained by calling the subroutine PLANE. The even-odd behavior in n of the coefficient of $e^{jn\phi_r}$ in (1-91) is as follows.

| Receiver Polarization | Transmitter Polarization | Behavior in n |
|---|---|---|
| $\theta$ | $\theta$ | even in n |
| $\phi$ | $\theta$ | odd in n |
| $\theta$ | $\phi$ | odd in n |
| $\phi$ | $\phi$ | even in n |

Here, the receiver polarization denotes the component of the far field being measured. The transmitter polarization is the polarization of the incident plane wave.

## II. THE SUBROUTINE ZMAT

The subroutine ZMAT(M1,M2,NP,NPHI,NT,RH,ZH,X,A,XT,AT,Z) calculates the moment matrices in (6) for n = M1,M1+1,...M2 where M1 $\geq$ 0 and stores them in Z. Z is the only output argument. The rest of the arguments of ZMAT are input arguments. For n = M1, storage of the $Z_n$ submatrices in Z is as follows.

$(Z_n^{tt})_{ij}$ in Z(i+N*(j-1))

$(Z_n^{\phi t})_{ij}$ in Z(i+N*(j-1) + NP-2)

$(Z_n^{t\phi})_{ij}$ in Z(i+N*(j-1) + (NP-2)*N)

$(Z_n^{\phi\phi})_{ij}$ in Z(i+N*(j-1) + (NP-2)*N+NP-2)

Here,

$$N = 2*NP-3 \tag{142}$$

For n > M1, the $Z_n$ submatrices are stored in Z((n-M1)*N*N+1) to Z((n-M1+1)*N*N) in the same manner as the $Z_n$ submatrices were stored in Z(1) to Z(N*N) for n = M1. Table 1 relates the third to eleventh arguments of ZMAT to variables in Part One of the text. In Table 1, $\rho(t_i^-)$ and $z(t_i^-)$ are the values of $\rho$ and z at $t = t_i^-$ for i = 1,2,...P.

Table 1. Third to eleventh arguments of ZMAT.

| Argument of ZMAT | Variables in Part One |
|---|---|
| NP | P |
| NPHI | $n_\phi$ |
| NT | $n_t$ |
| RH | $k\rho(\bar{t_1}),\ k\rho(\bar{t_2}), \ldots k\rho(\bar{t_P})$ |
| ZH | $kz(\bar{t_1}),\ kz(\bar{t_2}), \ldots kz(\bar{t_P})$ |
| X | $x_1^{(n_\phi)},\ x_2^{(n_\phi)}, \ldots x_{n_\phi}^{(n_\phi)}$ |
| A | $A_1^{(n_\phi)},\ A_2^{(n_\phi)}, \ldots A_{n_\phi}^{(n_\phi)}$ |
| XT | $x_1^{(n_t)},\ x_2^{(n_t)}, \ldots x_{n_t}^{(n_t)}$ |
| AT | $A_1^{(n_t)},\ A_2^{(n_t)}, \ldots A_{n_t}^{(n_t)}$ |

Minimum allocations are given by

```
COMPLEX Z(M3*N*N), G4A(M3), G5A(M3), G6A(M3),
     G4B(M3), G5B(M3), G6B(M3), GA(NPHI), GB(NPHI)
DIMENSION RH(NP), ZH(NP), X(NPHI), A(NPHI),
     XT(NT), AT(NT), RS(NP-1), ZS(NP-1), D(NP-1),
     DR(NP-1), DZ(NP-1), DM(NP-1), C2(NPHI),
     C3(NPHI), R2(NT), Z2(NT), C4(M3*NPHI), C5(M3*NPHI),
     C6(M3*NPHI), Z7(NT), R7(NT), Z8(NT), R8(NT)
```

where M3 = M2-M1+1.

The elements of the $Z_n$ submatrices are calculated according to (48)-(51) where $G_{ma}$ and $G_{mb}$ are given by (54), (55), and (62)-(66). However, (62)-(66) are modified through the use of methods 1, 2, or 3 in the cases specified by (105)-(107). The values of $c_t$ and $c_\phi$ suggested in (104) enter via CT and CP in lines 10 and 11.

DO loop 10 sets

$$RS(q) = k\rho_q \qquad DR(q) = \frac{k\Delta_q}{2} \sin v_q$$

$$ZS(q) = kz_q \qquad DZ(q) = \frac{k\Delta_q}{2} \cos v_q$$

$$D(q) = \frac{k\Delta_q}{2} \qquad DM(q) = \frac{\Delta_q}{2\rho_q}$$

for q = 1,2,... NP-1.

DO loop 11 sets

$$C2(K) = \phi_K^2 \quad \text{and} \quad C3(K) = 4 \sin^2(\frac{\phi_K}{2}).$$

Inner DO loop 29 sets

$$C4(M5) = \pi A_K^{(n_\phi)} \sin^2(\frac{\phi_K}{2}) \cos(n\phi_K)$$

$$C5(M5) = \frac{\pi}{2} A_K^{(n_\phi)} \cos \phi_K \cos(n\phi_K)$$

$$C6(M5) = \frac{\pi}{2} A_K^{(n_\phi)} \sin \phi_K \sin(n\phi_K)$$

where M5 = K + (n-M1)*NPHI.

The calculation of (48)-(51) occurs inside three DO loops nested in the following manner.

```
DO 15 JQ = 1, MP
DO 16 IP = 1, MP
DO 31  M = 1, M3
CALCULATION OF (48)-(51)
```

```
31    CONTINUE
16    CONTINUE
15    CONTINUE
```

Here, JQ, IP, and M represent, respectively, the variables q, p, and (n-M1+1) in (48)-(51). The JN introduced in line 52 is incremented in line 314 so that the subscript for $(Z_n^{tt})_{p-1,q-1}$ can be written as p + JN when n = M1. The variable KQ defined in lines 54 to 56 keeps track of the cases for which q = 1 and q = MP. Because of (24), these cases require special treatment. According to (24), expressions (48) and (49) are absent when j = q-1 and q = 1. Likewise, (48) and (49) are absent when j = q and q = MP.

The variables defined in statements 57 to 70 are needed inside DO loop 12 or DO loop 16. DO loop 12 puts $k\rho'$ and $kz'$ of (68) and (69) in R2 and Z2, respectively. To reduce execution time, references to subscripted variables as well as calculations are being done outside DO loops whenever possible. Unfortunately, this usually increases the number of statements and complicates the logic because factors such as $\frac{jk^2\Delta_p\Delta_q}{8}\sin v_p \sin v_q$ in (48) are computed by means of several statements scattered throughout the program. One way to follow the gradual building up of constants from outer to inner DO loops is to tabulate computer program variables versus variables in Part One of the text.

Lines 78 to 88 put $kd_o$ of (102) in D6. Lines 89 to 94 set KP equal to the case number in (103) and (105)-(107).

Lines 96 to 248 put approximate values of $G_{ma}$ of (56) in GmA for m = 4,5,6. Lines 96 to 248 also put approximate values of $G_{mb}$ of (57) in GmB for m = 4,5,6.

Lines 96 to 174 are executed for case 2 of (105) and for case 4 of (107). Method 1 is used here. This method is described by (71)-(93). The pure Gaussian quadrature option for $G_a$ and $G_b$ advocated just after (93) is

$$G_a = \sum_{\ell'=1}^{n_t} A_{\ell'}^{(n_t)} \frac{e^{-jkR_p}}{kR_p} \tag{143}$$

$$G_b = \sum_{\ell'=1}^{n_t} A_{\ell'}^{(n_t)} \; x_{\ell'}^{(n_t)} \frac{e^{-jkR_p}}{kR_p} \tag{144}$$

where $R_p$ has the same meaning as in (81). In terms of Z7, R7, Z8, and R8 calculated by DO loop 40,

$$kR_p = \sqrt{Z7(\ell') + R7(\ell')*(4 \sin^2(\frac{\phi}{2}))} \tag{145}$$

$$\frac{kR_p}{2} = \sqrt{Z8(\ell') + R8(\ell')*(4 \sin^2(\frac{\phi}{2}))} \tag{146}$$

DO loop 33 puts $G_a$ and $G_b$ in GA(K) and GB(K). The index K of DO loop 33 corresponds to $\ell$ in (91)-(93). Line 109 puts $k^2 r_{pq}^2$ of (86) in RR. If

$$r_{pq} < \frac{1}{2} c_t \Delta_q + \frac{1}{2} \Delta_q \tag{147}$$

then line 112 sends execution to statement 34 and $G_a$ and $G_b$ are calculated according to (73) and (74). Otherwise, DO loop 35 accumulates $G_a$ and $G_b$ of (143) and (144) in UA and UB. The purpose of the second

term on the right-hand side of (147) is to assure that the distance between the field point and the closest point on the line $\phi = \phi_K$ on the qth source segment is no less than $\frac{1}{2} c_t \Delta_q$ before DO loop 35 is entered. This distance could be as small as $r_{pq} - \frac{1}{2} \Delta_q$. DO loop 37 accumulates $G_{a1}$ and $G_{b1}$ of (79) and (80) in UA and UB. Lines 130 to 142 add $G_{a2}$ and $G_{b2}$ of (87) and (90) to UA and UB. Nested DO loops 45 and 46 put $G_{ma}$ of (91)-(93) in GmA for m = 4,5,6. These DO loops also put $G_{mb}$ in GmB for m = 4,5,6. The DO loop indices M and K correspond, respectively, to (n-M1+1) and $\ell$ in (91).

Lines 176 to 197 apply method 3 to $G_{5a}$. Expression (97) for $G_{5a}$ consists of three terms, namely, two double sums and a double integral. Since the first term in (97) is the result of pure Gaussian quadrature, the second and third terms in (97) are attributed to method 3. At this point, however, we do not have the first term in (97), but the modification of it due to application of method 1 in lines 96 to 174. For consistency, the inner sum in the second term in (97) should be replaced by the corresponding exact integral whenever (147) is true. This corresponding exact integral is given by

$$\frac{2}{k\Delta_q} \int_{-\frac{1}{2}\Delta_q}^{\frac{1}{2}\Delta_q} \frac{dt'}{\sqrt{t'^2 + \rho_q^2 \phi_\ell^2}} = \frac{4}{k\Delta_q} \log\left[ \frac{\Delta_q}{2\rho_q \phi_\ell} + \sqrt{1 + \left(\frac{\Delta_q}{2\rho_q \phi_\ell}\right)^2}\right] \tag{148}$$

Formula 200.01. of Dwight [6] was used to obtain the right-hand side of (148). The index K of DO loop 63 corresponds to $\ell$ in (97). Inner DO loop 65 accumulates in D7 the inner sum in the second term in (97).

Lines 188 and 189 put (148) in D7. Line 194 puts in D8 the contribution due to the second and third terms in (97). DO loop 67 adds this contribution to the modified first term in (97).

Lines 199 to 248 calculate $G_{ma}$ and $G_{mb}$ according to (62), (63), (64), (66) and either (65) or (94). The index L of outer DO loop 13 corresponds to $\ell'$ in (62) and (63). DO loop 17 puts $(e^{-jkR_{p\ell'\ell}})/(kR_{p\ell'\ell})$ in GA(K) for $\ell = K$. If, in accordance with (106),

$$c_\phi \rho_q > \sqrt{(\rho' - \rho_p)^2 + (z' - z_p)^2} \tag{149}$$

then (94) is used. Otherwise, (65) is used. If (149) is not true, then line 220 sends execution to statement 51. Otherwise, lines 221 to 225 put in D6 the contribution due to the second and third terms in (94). Note that the first term in (94) is the right-hand side of (65). DO loop 32 accumulates (64), (65), and (66) in U5, U6, and U7, respectively.

Inside DO loop 31, lines 262 and 263 put $G_{7a}$ and $G_{7b}$ of (54) and (55) in H4A and H4B, respectively. Lines 268 to 274 calculate terms in (48)-(50). U5, U6, and U7 belong in (48), U8 and U9 in (49), and UC and UD in (50). The variables K1 to K8 defined in lines 275 to 282 give the locations in Z of the matrix elements referenced in (48)-(50). See Table 2. In Table 2, p and q run from 1 to MP except where otherwise indicated. The forbidden values of p and q in Table 2 are due to (23) and (24). The contributions (48)-(51) are accounted for in lines 283 to 310. In these lines, Z(K4), Z(K6) and Z(K8) are referenced for

Table 2. Storage of matrix elements in Z.

| Location in Z | Matrix Element | |
|---|---|---|
| Z(K1) | $(Z_n^{tt})_{p-1,q-1}$ | $p \neq 1,\ q \neq 1$ |
| Z(K2) | $(Z_n^{tt})_{p,q-1}$ | $p \neq MP,\ q \neq 1$ |
| Z(K3) | $(Z_n^{tt})_{p-1,q}$ | $p \neq 1,\ q \neq MP$ |
| Z(K4) | $(Z_n^{tt})_{p,q}$ | $p \neq MP,\ q \neq MP$ |
| Z(K5) | $(Z_n^{\phi t})_{p,q-1}$ | $q \neq 1$ |
| Z(K6) | $(Z_n^{\phi t})_{p,q}$ | $q \neq MP$ |
| Z(K7) | $(Z_n^{t\phi})_{p-1,q}$ | $p \neq 1$ |
| Z(K8) | $(Z_n^{t\phi})_{p,q}$ | $p \neq MP$ |

the first time, but the rest of the Z's are incremented. The branch statements interspersed from lines 283 to 306 are due to the forbidden values of p and q in Table 2. The seemingly muddled and repetitive nature of the Z's in lines 283 to 309 is the result of an effort to minimize the number of branch statements executed.

```
C     LISTING OF THE SUBROUTINE ZMAT
C     THE SUBROUTINE ZMAT CALLS THE FUNCTION BLOG
      SUBROUTINE ZMAT(M1,M2,NP,NPHI,NT,RH,ZH,X,A,XT,AT,Z)
      COMPLEX Z(1600),U1,U2,U3,U4,U5,U6,U7,U8,U9,UA,UB,G4A(10),G5A(10)
      COMPLEX CMPLX,G6A(10),G4B(10),G5B(10),G6B(10),H4A,H5A,H6A,H4B,H5B
      COMPLEX H6B,UC,UD,GA(48),GB(48)
      DIMENSION RH(43),ZH(43),X(48),A(48),XT(10),AT(10),RS(42),ZS(42)
      DIMENSION D(42),DR(42),DZ(42),DM(42),C2(48),C3(48),R2(10),Z2(10)
      DIMENSION C4(200),C5(200),C6(200),Z7(10),R7(10),Z8(10),R8(10)
      CT=2.
      CP=.1
      DO 10 I=2,NP
      I2=I-1
      RS(I2)=.5*(RH(I)+RH(I2))
      ZS(I2)=.5*(ZH(I)+ZH(I2))
      D1=.5*(RH(I)-RH(I2))
      D2=.5*(ZH(I)-ZH(I2))
      D(I2)=SQRT(D1*D1+D2*D2)
      DR(I2)=D1
      DZ(I2)=D2
      DM(I2)=D(I2)/RS(I2)
   10 CONTINUE
      M3=M2-M1+1
      M4=M1-1
      PI2=1.570796
      DO 11 K=1,NPHI
      PH=PI2*(X(K)+1.)
      C2(K)=PH*PH
      SN=SIN(.5*PH)
      C3(K)=4.*SN*SN
      A1=PI2*A(K)
      D4=.5*A1*C3(K)
      D5=A1*COS(PH)
      D6=A1*SIN(PH)
      M5=K
      DO 29 M=1,M3
      PHM=(M4+M)*PH
      A2=COS(PHM)
      C4(M5)=D4*A2
      C5(M5)=D5*A2
      C6(M5)=D6*SIN(PHM)
      M5=M5+NPHI
   29 CONTINUE
   11 CONTINUE
      MP=NP-1
      MT=MP-1
      N=MT+MP
      N2N=MT*N
      N2=N*N
      U1=(0.,.5)
      U2=(0.,2.)
      JN=-1-N
      DO 15 JQ=1,MP
      KQ=2
      IF(JQ.EQ.1) KQ=1
      IF(JQ.EQ.MP) KQ=3
      R1=RS(JQ)
      Z1=ZS(JQ)
      D1=D(JQ)
      D2=DR(JQ)
```

```
      D3=DZ(JQ)
      D4=D2/R1
      D5=DH(JQ)
      SV=D2/D1
      CV=D3/D1
      T6=CT*D1
      T62=T6+D1
      T62=T62*T62
      R6=CP*R1
      R62=R6*R6
      DO 12 L=1,NT
      R2(L)=R1+D2*XT(L)
      Z2(L)=Z1+D3*XT(L)
   12 CONTINUE
      U3=D2*U1
      U4=D3*U1
      DO 16 IP=1,NP
      R3=RS(IP)
      Z3=ZS(IP)
      R4=R1-R3
      Z4=Z1-Z3
      FM=R4*SV+Z4*CV
      PHM=ABS(FM)
      PH=ABS(R4*CV-Z4*SV)
      D6=PH
      IF(PHM.LE.D1) GO TO 26
      D6=PHM-D1
      D6=SQRT(D6*D6+PH*PH)
   26 IF(IP.EQ.JQ) GO TO 27
      KP=1
      IF(T6.GT.D6) KP=2
      IF(R6.GT.D6) KP=3
      GO TO 28
   27 KP=4
   28 GO TO (41,42,41,42),KP
   42 DO 40 L=1,NT
      D7=R2(L)-R3
      D8=Z2(L)-Z3
      Z7(L)=D7*D7+D8*D8
      R7(L)=R3*R2(L)
      Z8(L)=.25*Z7(L)
      R8(L)=.25*R7(L)
   40 CONTINUE
      Z4=R4*R4+Z4*Z4
      R4=R3*R1
      R5=.5*R3*SV
      DO 33 K=1,NPHI
      A1=C3(K)
      RR=Z4+R4*A1
      UA=0.
      UB=0.
      IF(RR.LT.T62) GO TO 34
      DO 35 L=1,NT
      R=SQRT(Z7(L)+R7(L)*A1)
      SN=-SIN(R)
      CS=COS(R)
      UC=AT(L)/R*CMPLX(CS,SN)
      UA=UA+UC
      UB=XT(L)*UC+UB
   35 CONTINUE
```

```
      GO TO 36
   34 DO 37 L=1,NT
      R=SQRT(Z8(L)+R8(L)*A1)
      SN=-SIN(R)
      CS=COS(R)
      UC=AT(L)/R*SN*CMPLX(-SN,CS)
      UA=UA+UC
      UB=XT(L)*UC+UB
   37 CONTINUE
      A2=FM+R5*A1
      D9=RR-A2*A2
      R=ABS(A2)
      D7=R-D1
      D8=R+D1
      D6=SQRT(D8*D8+D9)
      R=SQRT(D7*D7+D9)
      IF(D7.GE.0.) GO TO 38
      A1=ALOG((D8+D6)*(-D7+R)/D9)/D1
      GO TO 39
   38 A1=ALOG((D8+D6)/(D7+R))/D1
   39 UA=A1+UA
      UB=A2*(4./(D6+R)-A1)/D1+UB
   36 GA(K)=UA
      GB(K)=UB
   33 CONTINUE
      K1=0
      DO 45 M=1,N3
      H4A=0.
      H5A=0.
      H6A=0.
      H4B=0.
      H5B=0.
      H6B=0.
      DO 46 K=1,NPHI
      K1=K1+1
      D6=C4(K1)
      D7=C5(K1)
      D8=C6(K1)
      UA=GA(K)
      UB=GB(K)
      H4A=D6*UA+H4A
      H5A=D7*UA+H5A
      H6A=D8*UA+H6A
      H4B=D6*UB+H4B
      H5B=D7*UB+H5B
      H6B=D8*UB+H6B
   46 CONTINUE
      G4A(M)=H4A
      G5A(M)=H5A
      G6A(M)=H6A
      G4B(M)=H4B
      G5B(M)=H5B
      G6B(M)=H6B
   45 CONTINUE
      IF(KP.NE.4) GO TO 47
      A2=D1/(PI2*R1)
      D6=2./D1
      D8=0.
      DO 63 K=1,NPHI
      A1=R4*C2(K)
```

```
      R=R4*C3(K)
      IF(R.LT.T62) GO TO 64
      D7=0.
      DO 65 L=1,NT
      D7=D7+AT(L)/SQRT(Z7(L)+A1)
   65 CONTINUE
      GO TO 66
   64 A1=A2/(X(K)+1.)
      D7=D6*ALOG(A1+SQRT(1.+A1*A1))
   66 D8=D8+A(K)*D7
   63 CONTINUE
      A1=.5*A2
      A2=1./A1
      D8=-PI2*D8+2./R1*(BLOG(A2)+A2*BLOG(A1))
      DO 67 M=1,M3
      G5A(M)=D8+G5A(M)
   67 CONTINUE
      GO TO 47
   41 DO 25 M=1,M3
      G4A(M)=0.
      G5A(M)=0.
      G6A(M)=0.
      G4B(M)=0.
      G5B(M)=0.
      G6B(M)=0.
   25 CONTINUE
      DO 13 L=1,NT
      A1=R2(L)
      R4=A1-R3
      Z4=Z2(L)-Z3
      Z4=R4*R4+Z4*Z4
      R4=R3*A1
      DO 17 K=1,NPHI
      R=SQRT(Z4+R4*C3(K))
      SN=-SIN(R)
      CS=COS(R)
      GA(K)=CMPLX(CS,SN)/R
   17 CONTINUE
      D6=0.
      IF(R62.LE.Z4) GO TO 51
      DO 62 K=1,NPHI
      D6=D6+A(K)/SQRT(Z4+R4*C2(K))
   62 CONTINUE
      Z4=3.141593/SQRT(Z4/R4)
      D6=-PI2*D6+ALOG(Z4+SQRT(1.+Z4*Z4))/SQRT(R4)
   51 A1=AT(L)
      A2=XT(L)*A1
      K1=0
      DO 30 M=1,M3
      U5=0.
      U6=0.
      U7=0.
      DO 32 K=1,NPHI
      UA=GA(K)
      K1=K1+1
      U5=C4(K1)*UA+U5
      U6=C5(K1)*UA+U6
      U7=C6(K1)*UA+U7
   32 CONTINUE
      U6=D6+U6
```

```
      G4A(N)=A1*U5+G4A(N)
      G5A(N)=A1*U6+G5A(N)
      G6A(N)=A1*U7+G6A(N)
      G4B(N)=A2*U5+G4B(N)
      G5B(N)=A2*U6+G5B(N)
      G6B(N)=A2*U7+G6B(N)
   30 CONTINUE
   13 CONTINUE
   47 A1=DR(IP)
      UA=A1*U3
      UB=DZ(IP)*U4
      A2=D(IP)
      D6=-A2*D2
      D7=D1*A1
      D8=D1*A2
      JM=JN
      DO 31 N=1,N3
      FN=N4+N
      A1=FN*DN(IP)
      H5A=G5A(N)
      H5B=G5B(N)
      H4A=G4A(N)+H5A
      H4B=G4B(N)+H5B
      H6A=G6A(N)
      H6B=G6B(N)
      U7=UA*H5A+UB*H4A
      U8=UA*H5B+UB*H4B
      U5=U7-U8
      U6=U7+U8
      U7=-U1*H4A
      U8=D6*H6A
      U9=D6*H6B-A1*H4A
      UC=D7*(H6A+D4*H6B)
      UD=FN*D5*H4A
      K1=IP+JM
      K2=K1+1
      K3=K1+N
      K4=K2+N
      K5=K2+NT
      K6=K4+NT
      K7=K3+N2N
      K8=K4+N2N
      GO TO (18,20,19),KQ
   18 Z(K6)=U8+U9
      IF(IP.EQ.1) GO TO 21
      Z(K3)=Z(K3)+U6-U7
      Z(K7)=Z(K7)+UC-UD
      IF(IP.EQ.MP) GO TO 22
   21 Z(K4)=U6+U7
      Z(K8)=UC+UD
      GO TO 22
   19 Z(K5)=Z(K5)+U8-U9
      IF(IP.EQ.1) GO TO 23
      Z(K1)=Z(K1)+U5+U7
      Z(K7)=Z(K7)+UC-UD
      IF(IP.EQ.MP) GO TO 22
   23 Z(K2)=Z(K2)+U5-U7
      Z(K8)=UC+UD
      GO TO 22
   20 Z(K5)=Z(K5)+U8-U9
      Z(K6)=U8+U9
      IF(IP.EQ.1) GO TO 24
      Z(K1)=Z(K1)+U5+U7
      Z(K3)=Z(K3)+U6-U7
      Z(K7)=Z(K7)+UC-UD
      IF(IP.EQ.MP) GO TO 22
   24 Z(K2)=Z(K2)+U5-U7
      Z(K4)=U6+U7
      Z(K8)=UC+UD
   22 Z(K8+NT)=U2*(D8*(H5A+D4*H5B)-A1*UD)
      JM=JM+N2
   31 CONTINUE
   16 CONTINUE
      JN=JN+N
   15 CONTINUE
      RETURN
      END
```

## III. THE FUNCTION BLOG

The function BLOG(x) calculates $\log(x + \sqrt{1 + x^2})$ for $x \geq 0$. If x is appreciable compared to 1, the FORTRAN supplied subroutine for the logarithm suffices. However, if x is much smaller than 1, this subroutine fails because of excessive roundoff error. From formulas 700.1. and 706. of Dwight [6],

$$\log(x + \sqrt{1+x^2}) = x\left(1 - \frac{1}{2\cdot 3} x^2 + \frac{1\cdot 3}{2\cdot 4\cdot 5} x^4 - \frac{1\cdot 3\cdot 5}{2\cdot 4\cdot 6\cdot 7} x^6 + \ldots\right),\ x^2 < 1 \quad (150)$$

If $|x| \leq .1$, the approximation

$$\log(x + \sqrt{1+x^2}) = x\left(1 - \frac{x^2}{6} + \frac{3x^4}{40}\right) \quad (151)$$

incurs an error of less than one part in $10^7$. The function BLOG(x) uses the FORTRAN supplied subroutine for the logarithm for $x > .1$ and (151) for $x \leq .1$.

```
C     LISTING OF THE FUNCTION BLOG
      FUNCTION BLOG(X)
      IF(X.GT..1) GO TO 1
      X2=X*X
      BLOG=((.075*X2-.1666667)*X2+1.)*X
      RETURN
    1 BLCG=ALOG(X+SQRT(1.+X*X))
      RETURN
      END
```

## IV. THE SUBROUTINE PLANE

The subroutine PLANE(M1,M2,NF,NP,NT,RH,ZH,XT,AT,THR,R) calculates the elements of the plane wave excitation vectors according to (124)-(127) and (132)-(133) and stores them in R. R is the only output argument. The rest of the arguments of PLANE are input arguments. There are NF angles of incidence $\theta_t$ of (110) and n = M1, M1+1,...M2 where M1 $\geq$ 0. The Kth angle of incidence resides in THR(K) in radians. For the first angle of incidence and for n = M1, storage in R is as follows.

$$\begin{array}{lll} V_{ni}^{t\theta} & \text{in} & \text{R(i)} \\ -V_{ni}^{\phi\theta} & \text{in} & \text{R(i+NP-2)} \\ -V_{ni}^{t\phi} & \text{in} & \text{R(i+N)} \\ V_{ni}^{\phi\phi} & \text{in} & \text{R(i+N+NP-2)} \end{array} \tag{152}$$

Here,

$$N = 2*NP-3 \tag{153}$$

The minus signs are attached to $V_{ni}^{\phi\theta}$ and $V_{ni}^{t\phi}$ in (152) so that, according to (1-100) and (1-104), the vectors stored in R will be measurement vectors. For the Kth angle of incidence and for n $\geq$ M1, the storage arrangement of $V_{ni}^{t\theta}$, $-V_{ni}^{\phi\theta}$, $-V_{ni}^{t\phi}$, and $V_{ni}^{\phi\phi}$ is still the same as indicated above, but the storage area now extends from R(2*N*((K-1)*(M2-M1+1) + n-M1) + 1) to R(2*N*((K-1)*(M2-M1+1) + n-M1+1)) instead of from R(1) to R(2*N). Table 3 relates the fourth to ninth arguments of PLANE to variables in Part One of the text. In Table 3, $\rho(\bar{t}_i)$ and $z(\bar{t}_i)$ are the values of $\rho$ and z at t = $\bar{t}_i$ for i = 1,2,...P.

Table 3. Fourth to ninth arguments of PLANE

| Argument of PLANE | Variable in Part One |
|---|---|
| NP | P |
| NT | $n_T$ |
| RH | $k\rho(\bar{t}_1)$, $k\rho(\bar{t}_2)$,... $k\rho(\bar{t}_P)$ |
| ZH | $kz(\bar{t}_1)$, $kz(\bar{t}_2)$,... $kz(\bar{t}_P)$ |
| XT | $x_1^{(n_T)}$, $x_2^{(n_T)}$ ,... $x_{n_T}^{(n_T)}$ |
| AT | $A_1^{(n_T)}$, $A_2^{(n_T)}$ ,... $A_{n_T}^{(n_T)}$ . |

Minimum allocations are given by

```
COMPLEX R(2*N*NF*(M2-M1+1)), FA(M2+3), FB(M2+3)
DIMENSION RH(NP), ZH(NP), XT(NT), AT(NT),
     THR(NF), CS(NF), SN(NF), R2(NT), Z2(NT)
```

where N is given by (153).

The index IP of DO loop 12 obtains p in (124)-(127). DO loop 13 puts $\frac{k}{2}\hat{\rho}_\ell$ of (134) and $k\hat{z}_\ell$ of (135) in R2(L) and Z2(L), respectively, for $\ell$ = L. The index K of DO loop 14 obtains the Kth angle of incidence.

The index L of DO loop 15 obtains $\ell$ in (132) and (133). Line 48 puts $\frac{k}{2}\hat{\rho}_\ell \sin\theta_t$ in X. Lines 49 to 73 calculate S and BJ(m+2) so that

$$BJ(m+2) = S*J_m(k\hat{\rho}_\ell \sin \theta_t), \quad m = M1-1, M1, \ldots M2+1$$

$$m \neq -1$$

If the argument of the Bessel function $J_m$ in the above equation does not exceed $10^{-7}$, lines 50 to 54 use the approximations

$$J_m = \begin{cases} 0, & m \neq 0 \\ 1, & m = 0 \end{cases}$$

in order to obtain BJ(m+2) and S. The purpose of lines 56 and 57 is to obtain M so large that $|J_{M-2}(k\hat{\rho}_\ell \sin \theta_t)|$ is roughly $10^{-8}$. Line 58 assures that M is at least as large as M2+3. Lines 59 to 67 start with

$$J_{M-2}(x) = 0$$

$$J_{M-3}(x) = 1$$

and use the recurrence relation

$$J_{n-1}(x) = \frac{2n}{x} J_n(x) - J_{n+1}(x)$$

taken from (9.1.27) on page 361 of [12] to calculate $J_n(x)$ for n = M-4, M-5,... 0. Lines 68 to 73 use

$$1 = J_0(x) + 2J_2(x) + 2J_4(x) + 2J_6(x) + \ldots$$

taken from (9.1.46) on page 361 of [12] to obtain the normalization constant S. As the index of DO loop 15 changes, DO loop 25 accumulates $F_{ma}$ and $F_{mb}$ of (132) and (133) in FA(m+2) and FB(m+2), respectively. If $F_{-1,a}$ and $F_{-1,b}$ are needed, lines 83 and 84 use the formulas

$$F_{-1,a} = F_{1a}$$

$$F_{-1,b} = F_{1b}$$

to store $F_{-1,a}$ and $F_{-1,b}$ in FA(1) and FB(1), respectively.

With reference to (124)-(127), the index M of DO loop 27 obtains (n+2). Inside DO loop 27, UA is $\pi j^n$. The variables U2, U3, U4, and U5 calculated in lines 95 to 98 are needed in order to assemble the right-hand sides of (124) and (126). The variables K1, K2, K4, and K5 are the subscripts of R for $V^{t\theta}_{n,p-1}$, $V^{t\theta}_{np}$, $V^{t\phi}_{n,p-1}$ and $V^{t\phi}_{np}$, respectively. Lines 102 and 103 obtain (125) and (127). The branch statement in line 104 is necessary because neither $V^{t\theta}_{n,p-1}$ nor $V^{t\phi}_{n,p-1}$ exists for p=1. In lines 105 and 106, $V^{t\theta}_{n,p-1}$ and $V^{t\phi}_{n,p-1}$ are incremented. The branch statement in line 107 is necessary because neither $V^{t\theta}_{np}$ nor $V^{t\phi}_{np}$ exists for p = NP-1. In lines 108 and 109, $V^{t\theta}_{np}$ and $V^{t\phi}_{np}$ are referenced for the first time.

```
C     LISTING OF THE SUBROUTINE PLANE
      SUBROUTINE PLANE(M1,M2,NF,NP,NT,RH,ZH,XT,AT,THR,R)
      COMPLEX R(240),U,U1,UA,UB,FA(10),FB(10),F2A,F2B,F1A,F1B,U2,U3,U4
      COMPLEX U5,CMPLX
      DIMENSION RH(43),ZH(43),XT(10),AT(10),THR(3),CS(3),SN(3),R2(10)
      DIMENSION Z2(10),BJ(50)
      MP=NP-1
      NT=NP-1
      N=NT+MP
      N2=2*N
      DO 11 K=1,NF
      X=THR(K)
      CS(K)=COS(X)
      SN(K)=SIN(X)
   11 CONTINUE
      U=(0.,1.)
      U1=3.141593*U**M1
      M3=M1+1
      M4=M2+3
      IF(M1.EQ.0) M3=2
      M5=M1+2
      M6=M2+2
      DO 12 IP=1,MP
      K2=IP
      I=IP+1
      DR=.5*(RH(I)-RH(IP))
      DZ=.5*(ZH(I)-ZH(IP))
      D1=SQRT(DR*DR+DZ*DZ)
      R1=.25*(RH(I)+RH(IP))
      Z1=.5*(ZH(I)+ZH(IP))
      DR=.5*DR
      D2=DR/R1
      DO 13 L=1,NT
      R2(L)=R1+DR*XT(L)
      Z2(L)=Z1+DZ*XT(L)
   13 CONTINUE
      DO 14 K=1,NF
      CC=CS(K)
      SS=SN(K)
      D3=DR*CC
      D4=-DZ*SS
      D5=D1*CC
      DO 23 M=M3,M4
      FA(M)=0.
      FB(M)=0.
   23 CONTINUE
      DO 15 L=1,NT
      X=SS*R2(L)
      IF(X.GT..5E-7) GO TO 19
      DO 20 M=M3,M4
      BJ(M)=0.
   20 CONTINUE
      BJ(2)=1.
      S=1.
      GO TO 18
   19 M=2.8*X+14.-2./X
      IF(X.LT..5) M=11.8+ALOG10(X)
      IF(M.LT.M4) M=M4
      BJ(M)=0.
      JM=M-1
```

```
      BJ(JM)=1.
      DO 16 J=4,M
      J2=JM
      JM=JM-1
      J1=JM-1
      BJ(JM)=J1/X*BJ(J2)-BJ(JM+2)
   16 CONTINUE
      S=0.
      IF(M.LE.4) GO TO 24
      DO 17 J=4,M,2
      S=S+BJ(J)
   17 CONTINUE
   24 S=BJ(2)+2.*S
   18 ARG=Z2(L)*CC
      UA=AT(L)/S*CMPLX(COS(ARG),SIN(ARG))
      UB=XT(L)*UA
      DO 25 M=M3,M4
      FA(M)=BJ(M)*UA+FA(M)
      FB(M)=BJ(M)*UB+FB(M)
   25 CONTINUE
   15 CONTINUE
      IF(M1.NE.0) GO TO 26
      FA(1)=FA(3)
      FB(1)=FB(3)
   26 UA=U1
      DO 27 M=M5,M6
      M7=M-1
      M8=M+1
      F2A=UA*(FA(M8)+FA(M7))
      F2B=UA*(FB(M8)+FB(M7))
      UB=U*UA
      F1A=UB*(FA(M8)-FA(M7))
      F1B=UB*(FB(M8)-FB(M7))
      U4=D4*UA
      U2=D3*F1A+U4*FA(M)
      U3=D3*F1B+U4*FB(M)
      U4=DR*F2A
      U5=DR*F2B
      K1=K2-1
      K4=K1+N
      K5=K2+N
      R(K2+MT)=-D5*(F2A+D2*F2B)
      R(K5+MT)=D1*(F1A+D2*F1B)
      IF(IP.EQ.1) GO TO 21
      R(K1)=R(K1)+U2-U3
      R(K4)=R(K4)+U4-U5
      IF(IP.EQ.NP) GO TO 22
   21 R(K2)=U2+U3
      R(K5)=U4+U5
   22 K2=K2+N2
      UA=UB
   27 CONTINUE
   14 CONTINUE
   12 CONTINUE
      RETURN
      END
```

## V. THE SUBROUTINES DECOMP AND SOLVE

The subroutines DECOMP(N, IPS, UL) and SOLVE(N, IPS, UL, B, X) solve a system of N linear equations in N unknowns. The input to DECOMP consists of N and the N by N matrix of coefficients on the left-hand side of the matrix equation stored by columns in UL. The output from DECOMP is IPS and UL. This output is fed into SOLVE. The rest of the input to SOLVE consists of N and the column of coefficients on the right-hand side of the matrix equation stored in B. SOLVE puts the solution to the matrix equation in X.

Minimum allocations are given by

```
COMPLEX UL(N*N)
DIMENSION SCL(N), IPS(N)
```

in DECOMP and by

```
COMPLEX UL(N*N), B(N), X(N)
DIMENSION IPS(N)
```

in SOLVE.

More detail concerning DECOMP and SOLVE is on pages 46-49 of [13].

```
C     LISTING OF THE SUBROUTINES DECOMP AND SOLVE
      SUBROUTINE DECOMP(N,IPS,UL)
      COMPLEX UL(1600),PIVOT,EM
      DIMENSION SCL(40),IPS(40)
      DO 5 I=1,N
      IPS(I)=I
      RN=0.
      J1=I
      DO 2 J=1,N
      ULM=ABS(REAL(UL(J1)))+ABS(AIMAG(UL(J1)))
      J1=J1+N
      IF(RN-ULM) 1,2,2
    1 RN=ULM
    2 CONTINUE
      SCL(I)=1./RN
    5 CONTINUE
      NM1=N-1
      K2=0
      DO 17 K=1,NM1
      BIG=0.
      DO 11 I=K,N
      IP=IPS(I)
      IPK=IP+K2
      SIZE=(ABS(REAL(UL(IPK)))+ABS(AIMAG(UL(IPK))))*SCL(IP)
      IF(SIZE-BIG) 11,11,10
   10 BIG=SIZE
      IPV=I
   11 CONTINUE
      IF(IPV-K) 14,15,14
   14 J=IPS(K)
      IPS(K)=IPS(IPV)
      IPS(IPV)=J
   15 KPP=IPS(K)+K2
      PIVOT=UL(KPP)
      KP1=K+1
      DO 16 I=KP1,N
      KP=KPP
      IP=IPS(I)+K2
      EM=-UL(IP)/PIVOT
   18 UL(IP)=-EM
      DO 16 J=KP1,N
      IP=IP+N
      KP=KP+N
      UL(IP)=UL(IP)+EM*UL(KP)
   16 CONTINUE
      K2=K2+N
   17 CONTINUE
      RETURN
      END
      SUBROUTINE SOLVE(N,IPS,UL,B,X)
      COMPLEX UL(1600),B(40),X(40),SUM
      DIMENSION IPS(40)
      NP1=N+1
      IP=IPS(1)
      X(1)=B(IP)
      DO 2 I=2,N
      IP=IPS(I)
      IPB=IP
      IM1=I-1
      SUM=0.
      DO 1 J=1,IM1
      SUM=SUM+UL(IP)*X(J)
    1 IP=IP+N
    2 X(I)=B(IPB)-SUM
      K2=N*(N-1)
      IP=IPS(N)+K2
      X(N)=X(N)/UL(IP)
      DO 4 IBACK=2,N
      I=NP1-IBACK
      K2=K2-N
      IPI=IPS(I)+K2
      IP1=I+1
      SUM=0.
      IP=IPI
      DO 3 J=IP1,N
      IP=IP+N
    3 SUM=SUM+UL(IP)*X(J)
    4 X(I)=(X(I)-SUM)/UL(IPI)
      RETURN
      END
```

## VI. THE MAIN PROGRAM

The main program calculates the electric current induced by a plane wave axially incident on a perfectly conducting surface of revolution. This plane wave is given by (108) with $\theta_t = 0$ or $\pi$ radians. The components of the electric current are obtained from (140) and (141) in which $I_{1p}^t$ and $I_{1p}^\phi$ are the pth elements of the vectors $\vec{I}_1^t$ and $\vec{I}_1^\phi$ which satisfy (6) for n=1.

Punched card data are read in according to

```
      READ(1,15) NT, NPHI
15    FORMAT(2I3)
      READ(1,10)(XT(K), K=1, NT)
      READ(1,10)(AT(K), K=1, NT)
10    FORMAT(5E14.7)
      READ(1,10)(X(K), K=1, NPHI)
      READ(1,10)(A(K), K=1, NPHI)
      READ(1,16) NP, BK, THR(1)
16    FORMAT(I3, 2E14.7)
      READ(1,18)(RH(I), I=1, NP)
      READ(1,18)(ZH(I), I=1, NP)
18    FORMAT(10F8.4)
```

Here, BK is the propagation constant k and THR(1) is the angle of incidence $\theta_t$ in radians. THR(1) must be either 0 or $\pi$. The input variables NT, NPHI, XT, AT, X, A, and NP are defined in Table 1. These input variables can therefore be fed directly into the subroutine ZMAT. However, RH and ZH must be multiplied by BK before being fed

into ZMAT. More precisely, RH and ZH are values of $\rho$ and z so that the product of RH with BK is the RH in Table 1, and the product of ZH with BK is the ZH in Table 1. The sample input and output data listed along with the main program are for the spherical shell of Fig. 10.

Minimum allocations are given by

```
COMPLEX Z(N*N), R(2*N), B(N), C(N)
DIMENSION RH(NP), ZH(NP), X(NPHI),
  A(NPHI), XT(NT), AT(NT), IPS(N)
```

where N = 2*NP-3.

With reference to (6), line 41 puts the moment matrix in Z. Line 46 puts the excitation vector $\vec{V}_1^t$ of (6) and the negative of the excitation vector $\vec{V}_1^\phi$ of (6) in R(1) to R(2*NP-3). These excitation vectors are for the $\theta$-polarized plane wave (108) and their elements are called $V_{1i}^{t\theta}$ and $V_{1i}^{\phi\theta}$. Storage in R is according to (152). Now, $-V_{1i}^{t\phi}$ and $V_{1i}^{\phi\phi}$ are also stored in R, but are not used. Lines 47 to 52 put $\vec{V}_1^t$ and $\vec{V}_1^\phi$ in B. Lines 55 and 56 put the solution vectors $\vec{I}_1^t$ and $\vec{I}_1^\phi$ to (6) in C. DO loop 24 prints out (140) at $\phi = 0°$. DO loop 27 prints out (141) at $\phi = 90°$.

```
C       LISTING OF THE MAIN PROGRAM
C       THE SUBROUTINES ZMAT, PLANE, DECOMP, AND SOLVE ARE CALLED.
//PGM JOB (XXXX,XXXX,1,2),'MAUTZ,JOE',REGION=200K
// EXEC WATFIV
//GO.SYSIN DD *
$JOB             MAUTZ,TIME=5,PAGES=60
        COMPLEX Z(1600),R(240),B(40),C(40),U,CI
        DIMENSION THR(3),RH(43),ZH(43),X(48),A(48),XT(10),AT(10),IPS(40)
        READ(1,15) NT,NPHI
     15 FORMAT(2I3)
        WRITE(3,30) NT,NPHI
     30 FORMAT('  NT NPHI'/1X,I3,I5)
        READ(1,10)(XT(K),K=1,NT)
        READ(1,10)(AT(K),K=1,NT)
     10 FORMAT(5E14.7)
        WRITE(3,11)(XT(K),K=1,NT)
        WRITE(3,12)(AT(K),K=1,NT)
     11 FORMAT(' XT'/(1X,5E14.7))
     12 FORMAT(' AT'/(1X,5E14.7))
        READ(1,10)(X(K),K=1,NPHI)
        READ(1,10)(A(K),K=1,NPHI)
        WRITE(3,13)(X(K),K=1,NPHI)
        WRITE(3,14)(A(K),K=1,NPHI)
     13 FORMAT(' X'/(1X,5E14.7))
     14 FORMAT(' A'/(1X,5E14.7))
        READ(1,16) NP,BK,THR(1)
     16 FORMAT(I3,2E14.7)
        WRITE(3,17) NP,BK,THR(1)
     17 FORMAT('  NP',6X,'BK',12X,'THR'/1X,I3,2E14.7)
        READ(1,18)(RH(I),I=1,NP)
        READ(1,18)(ZH(I),I=1,NP)
     18 FORMAT(10F8.4)
        WRITE(3,19)(RH(I),I=1,NP)
        WRITE(3,20)(ZH(I),I=1,NP)
     19 FORMAT(' RH'/(1X,10F8.4))
     20 FORMAT(' ZH'/(1X,10F8.4))
        DO 28 J=1,NP
        RH(J)=BK*RH(J)
        ZH(J)=BK*ZH(J)
     28 CONTINUE
        CALL ZMAT(1,1,NP,NPHI,NT,RH,ZH,X,A,XT,AT,Z)
        MT=NP-2
        N=2*MT+1
        WRITE(3,29)(Z(J),J=1,N)
     29 FORMAT(' Z'/(1X,6E11.4))
        CALL PLANE(1,1,1,NP,NT,RH,ZH,XT,AT,THR,R)
        DO 22 J=1,MT
        B(J)=R(J)
        J1=J+MT
        B(J1)=-R(J1)
     22 CONTINUE
        B(N)=-R(N)
        WRITE(3,23)(B(J),J=1,N)
     23 FORMAT(' B'/(1X,6E11.4))
        CALL DECOMP(N,IPS,Z)
        CALL SOLVE(N,IPS,Z,B,C)
        U=(0.,1.)
        WRITE(3,21)
     21 FORMAT('      REAL JT      IMAG JT       MAG JT')
        DO 24 J=1,MT
```

```
      C1=2./RH(J+1)*C(J)
      C2=CABS(C1)
      WRITE(3,25) C1,C2
   25 FORMAT(1X,3E11.4)
   24 CONTINUE
      WRITE(3,26)
   26 FORMAT('     REAL JP      IMAG JP       MAG JP')
      NP=NP-1
      DO 27 J=1,NP
      C1=4./(RH(J)+RH(J+1))*U*C(J+NT)
      C2=CABS(C1)
      WRITE(3,25) C1,C2
   27 CONTINUE
      STOP
      END
$DATA
  2 20
-0.5773503E+00 0.5773503E+00
 0.1000000E+01 0.1000000E+01
-0.9931286E+00-0.9639719E+00-0.9122344E+00-0.8391170E+00-0.7463319E+00
-0.6360537E+00-0.5108670E+00-0.3737061E+00-0.2277859E+00-0.7652652E-01
 0.7652652E-01 0.2277859E+00 0.3737061E+00 0.5108670E+00 0.6360537E+00
 0.7463319E+00 0.8391170E+00 0.9122344E+00 0.9639719E+00 0.9931286E+00
 0.1761401E-01 0.4060143E-01 0.6267205E-01 0.8327674E-01 0.1019301E+00
 0.1181945E+00 0.1316886E+00 0.1420961E+00 0.1491730E+00 0.1527534E+00
 0.1527534E+00 0.1491730E+00 0.1420961E+00 0.1316886E+00 0.1181945E+00
 0.1019301E+00 0.8327674E-01 0.6267205E-01 0.4060143E-01 0.1761401E-01
 11 0.1256637E+01 0.0000000E+00
  0.0000  0.2334  0.4540  0.6494  0.8090  0.9239  0.9877  0.9969  0.9511  0.8526
  0.7071
 -1.0000 -0.9724 -0.8910 -0.7604 -0.5878 -0.3827 -0.1564  0.0785  0.3090  0.5225
  0.7071
$STOP
/*
//
PRINTED OUTPUT
 NT NPHI
  2   20
XT
-0.5773503E+00 0.5773503E+00
AT
 0.1000000E+01 0.1000000E+01
X
-0.9931286E+00-0.9639719E+00-0.9122344E+00-0.8391170E+00-0.7463319E+00
-0.6360537E+00-0.5108670E+00-0.3737061E+00-0.2277859E+00-0.7652652E-01
 0.7652652E-01 0.2277859E+00 0.3737061E+00 0.5108670E+00 0.6360537E+00
 0.7463319E+00 0.8391170E+00 0.9122344E+00 0.9639719E+00 0.9931286E+00
A
 0.1761401E-01 0.4060143E-01 0.6267208E-01 0.8327675E-01 0.1019301E+00
 0.1181945E+00 0.1316886E+00 0.1420961E+00 0.1491730E+00 0.1527534E+00
 0.1527534E+00 0.1491730E+00 0.1420961E+00 0.1316886E+00 0.1181945E+00
 0.1019301E+00 0.8327675E-01 0.6267208E-01 0.4060143E-01 0.1761401E-01
 NP      BK           THR
 11 0.1256637E+01 0.0000000E+00
RH
  0.0000  0.2334  0.4540  0.6494  0.8090  0.9239  0.9877  0.9969  0.9511  0.8526
  0.7071
ZH
 -1.0000 -0.9724 -0.8910 -0.7604 -0.5878 -0.3827 -0.1564  0.0785  0.3090  0.5225
  0.7071
```

```
Z
 0.8363E-01-0.9778E+01 0.7552E-01 0.2574E+01 0.6344E-01 0.7723E+00
 0.4919E-01 0.2893E+00 0.3460E-01 0.1491E+00 0.2126E-01 0.9127E-01
 0.1024E-01 0.6477E-01 0.1954E-02 0.5293E-01-0.3673E-02 0.4842E-01
-0.1348E+02 0.8701E-01 0.2413E+01 0.8414E-01 0.4250E+00 0.7858E-01
 0.1369E+00 0.7103E-01 0.7633E-01 0.6213E-01 0.5943E-01 0.5265E-01
 0.5437E-01 0.4326E-01 0.5275E-01 0.3455E-01 0.5202E-01 0.2694E-01
 0.5134E-01 0.2063E-01
B
 0.3151E+00-0.8385E+00 0.3631E+00-0.7352E+00 0.4046E+00-0.5696E+00
 0.3966E+00-0.3656E+00 0.3074E+00-0.1689E+00 0.1384E+00-0.3786E-01
-0.7037E-01-0.1748E-01-0.2587E+00-0.1152E+00-0.3766E+00-0.2963E+00
 0.8755E+00 0.3070E+00 0.8527E+00 0.3660E+00 0.7959E+00 0.4749E+00
 0.6917E+00 0.6161E+00 0.5279E+00 0.7602E+00 0.3060E+00 0.8730E+00
 0.4503E-01 0.9236E+00-0.2219E+00 0.8975E+00-0.4598E+00 0.8031E+00
-0.6438E+00 0.6653E+00
   REAL JT    IMAG JT     MAG JT
 0.1142E+01 0.1198E+01 0.1655E+01
 0.8187E+00 0.1199E+01 0.1451E+01
 0.3432E+00 0.1163E+01 0.1212E+01
-0.2206E+00 0.1035E+01 0.1058E+01
-0.7768E+00 0.7827E+00 0.1103E+01
-0.1222E+01 0.4161E+00 0.1291E+01
-0.1474E+01-0.6146E-02 0.1474E+01
-0.1489E+01-0.3877E+00 0.1538E+01
-0.1248E+01-0.6133E+00 0.1391E+01
   REAL JP    IMAG JP     MAG JP
-0.1209E+01-0.1184E+01 0.1692E+01
-0.1076E+01-0.1094E+01 0.1534E+01
-0.9486E+00-0.9418E+00 0.1337E+01
-0.8584E+00-0.7213E+00 0.1121E+01
-0.8928E+00-0.4863E+00 0.1017E+01
-0.1102E+01-0.3341E+00 0.1152E+01
-0.1480E+01-0.3804E+00 0.1528E+01
-0.2002E+01-0.7355E+00 0.2133E+01
-0.2629E+01-0.1433E+01 0.2995E+01
-0.6381E+01-0.5179E+01 0.8219E+01
```

## REFERENCES


[1] J. R. Mautz and R. F. Harrington, "H-Field, E-Field, and Combined Field Solutions for Bodies of Revolution," Report RADC-TR-77-109, N.T.I.S. No. ADA 040379, Rome Air Development Center, Griffiss Air Force Base, N.Y., June 1977, A040379.

[2] A. W. Glisson and D. R. Wilton, "Simple and Efficient Numerical Techniques for Treating Bodies of Revolution," Report RADC-TR-79-22, N.T.I.S. No. ADA 067361, Rome Air Development Center, Griffiss Air Force Base, New York, March 1979, A067361.

[3] P. J. Davis and P. Rabinowitz, Methods of Numerical Integration, Academic Press, 1975, p. 139.

[4] J. Meixner, "The Behavior of Electromagnetic Fields at Edges," IEEE Trans. Antennas Propagat., vol. AP-20, No. 4, pp. 442-446. July 1972.

[5] V. I. Krylov, Approximate Calculation of Integrals, translated by A. H. Stroud, Macmillan Co., New York, 1962.

[6] H. B. Dwight, Tables of Integrals and Other Mathematical Data, Macmillan, New York, 1961.

[7] C. Cha and R. F. Harrington, "Electromagnetic Transmission through an Annular Aperture in an Infinite Conducting Screen," S.U. Report TR-79-11, N.T.I.S. No. ADA 074831, Department of Electrical and Computer Engineering, Syracuse University, Syracuse, NY. Sept. 1979.

[8] R. F. Harrington and J. R. Mautz, "Radiation and Scattering from Bodies of Revolution," Report AFCRL-69-0305, N.T.I.S. No. AD 859670, Contract No. F-19628-67-C-0233 between Syracuse University and Air Force Cambridge Research Laboratories, July 1969.

[9] A. J. Poggio and E. K. Miller, "Integral Equation Solutions of Three-dimensional Scattering Problems," Chapt. 4 of Computer Techniques for Electromagnetics, edited by R. Mittra, Pergamon Press, 1973.

[10] W. A. Davis and R. Mittra, "A New Approach to the Thin Scatterer Problem Using the Hybrid Equations," IEEE Trans. Antennas Propagation, vol. AP-25, No. 3, pp. 402-406, May 1977.

[11] C. J. Bouwkamp, "On the Diffraction of Electromagnetic Waves by Small Circular Disks and Holes," Philips Res. Rep., vol. 5, pp. 401-422, December 1950.

[12] M. Abramowitz and I. A. Stegun, "Handbook of Mathematical Functions," U.S. Government Printing Office, Washington, D.C. (Natl. Bur. Std. U.S. Applied Math. Ser. 55), 1964.

[13] J. R. Mautz and R. F. Harrington, "Transmission from a Rectangular Waveguide into Half Space Through a Rectangular Aperture," Interim Technical Report RADC-TR-76-264, N.T.I.S. No. ADA 030779, Rome Air Development Center, Griffiss Air Force Base, New York, August 1976, A030779.